AIMS Mathematics, 11(2): 5246–5269.
DOI: 10.3934/math.2026215
Received: 08 October 2025
Revised: 16 January 2026
Accepted: 20 January 2026
Published: 28 February 2026

https://www.aimspress.com/journal/Math

Research article

An operational treatment for two-dimensional time-fractional Gray-Scott models

Samer S. Ezz-Eldien[1,2,*], Ali H. Tedjani[3], Amra Al Kenany[4] and Marwa Alzubaidi[5]

[1] Department of Mathematics, Faculty of Science, New Valley University, El-Kharga, 72511, Egypt

[2] Department of İnformation Technology, Faculty of Computer and İnformation, Archipelago University, Socotra, Yemen

[3] Department of Mathematics and Statistics, College of Science, Imam Mohammad Ibn Saud Islamic University (IMSIU), Riyadh, Saudi Arabia

[4] Mathematics Department, Al-Qunfudah University College, Umm Al-Qura University, Mecca, KSA

[5] Department of Mathematics, Faculty of Science, University of Tabuk, Tabuk 71491, Saudi Arabia

* **Correspondence:** Email: s_sezeldien@yahoo.com.

Abstract: Due to the poor regularity of solutions to time-fractional partial differential equations, traditional spectral approaches typically suffer from significant accuracy reductions when applied in the time domain. To overcome this problem, in this paper, we applied a spectral approach based on a new set of basis functions, which are smooth in the spatial direction and non-smooth in the time direction. The spectral collocation approach was used combined with the operational matrix approach based on the new set of basis functions to solve two-dimensional time-fractional Gray-Scott models. Applying the operational technique reduces the computations of the full scheme and achieves significant accuracy by using a small number of these functions. Numerical results confirmed the high accuracy of the proposed approach when applied for smooth and non-smooth solutions.

Keywords: Legendre polynomial; spectral collocation method; operational matrix; fractional differential equations; Gray-Scott model
Mathematics Subject Classification: 65L05, 65R20, 65N35, 65L03

1. Introduction

The reaction-diffusion model is a special case of partial differential equations that captures the dynamic interactions between reactants, diffusers, and carriers. It has been widely used in diverse

fields, including the dispersion of drugs in biological environments, the flow of groundwater to purification systems, and many other chemical reactions [1, 2]. In addition, the reaction–diffusion framework is a valuable analytical tool in multiple disciplines, including ecology, sociology, chemistry, and biology, particularly in the investigation of pattern formation [3–5]. This framework has the potential to investigate natural patterns observed in different organisms, including leopards, seashells, and snakes [6, 7], and also makes a significant contribution to describing the spatial distribution of viruses such as hepatitis B [8]. These models have broad applications in practical life, such as biological sciences, heat transfer, and electromagnetism [9, 10]. In 1983, Gray and Scott introduced the Gray-Scott model, a widely used reaction-diffusion model that explains various types of space-time patterns that occur in real life. These patterns encompass a wide range of important phenomena, including spots, self-propagating waves, and other complex systems. Thanks to its high importance, the Gray–Scott model has been used as an effective instrument for explaining the complex behaviors of chemical reactions and pattern formation [11–13].

In most practical applications, traditional diffusion assumptions fail due to media inhomogeneity or memory effects. To overcome this problem, fractional-order models, which incorporate fractional-order derivatives, have received significant attention for their ability to describe subdiffusive and anomalous diffusion behavior [14, 15]. In this regard, the fractional-order Gray-Scott model extends the well-known one by replacing first-order time derivatives or second-order spatial derivatives with a fractional derivative. This modification enhances the model's realism and flexibility in describing pattern formation processes with anomalous diffusion behavior or temporal memory effects [16–18]. Wang et al. [19] used the fractional-order Gray-Scott model to study the effects of anomalous diffusion on pattern formation, and presented a semi-discrete numerical approach based on the weighted shifted Grunwald difference and Crank–Nicolson schemes in spatial and temporal discretizations, respectively. In [20], the authors presented a numerical technique for the space fractional Gray-Scott model using the Fourier transform method in the space direction, and the Runge-Kutta method in the time direction. The authors in [21] introduced a numerical scheme for a two-dimensional space fractional Gray-Scott model. They used a fourth-order compact difference approach to discretize the space fractional derivatives and the backward differentiation formula for the temporal discretization. Aljhani et al. [22] considered the time-fractional Gray-Scott model and utilized the fractional homotopy analysis transform technique to solve it. Sakariya and Kumar [23] implemented the spectral collocation approach based on radial basis functions and the finite difference approximation for space and time discretizations, respectively, to solve the two-dimensional time-fractional Gray-Scott model.

A major challenge in the numerical treatment of fractional differential equations lies in the intrinsic nonsmoothness of their solutions. Fractional operators often generate weak singularities and nonlocal behaviors that severely limit the performance of classical spectral and high-order methods, which typically rely on global smoothness assumptions. Addressing these fundamental difficulties, Zaky's works [24–27] introduced a unified fractional spectral philosophy that constructs basis functions tailored to the true analytical structure of fractional models. By embedding the expected singularity profiles directly into the basis itself, this framework, built upon fractional Jacobi polynomials, second-kind fractional Legendre functions, and other customized families, achieves high accuracy even for solutions with low regularity. These contributions provide a systematic strategy for overcoming the breakdown of conventional numerical schemes in fractional settings and establish a versatile foundation for developing robust, high-order algorithms across a wide class of fractional problems.

In this paper, we intend to present a numerical scheme for one- and two-dimensional time-fractional Gray-Scott models. We apply the spectral collocation method in both time and space directions combined with operational matrices of fractional- and second-order derivatives to simplify the model into a system of algebraic equations. To overcome the poor regularities caused by fractional-order derivatives in such models, we introduce a new set of basis functions—the fractional-order shifted Legendre function (FSLF) in one- and two-dimensions—which is smooth in the spatial directions and non-smooth in the time direction. The poor regularity of the FSLFs in the time direction effectively captures the singularity of solutions near the initial time, which in turn enhances the numerical accuracy of the numerical approach compared to the same approach based on the classical basis. One- and two-dimensional FSLFs are formulated based on the classical shifted Legendre orthogonal polynomials, and the application of operational matrix approaches based on this basis improves the numerical results of such approaches. The key contributions of this study are summarized below:

- We introduce a new family of one- and two-dimensional fractional-order shifted Legendre functions (FSLFs) and derive, for the first time, their complete operational matrices for second-order spatial derivatives and Caputo fractional time derivatives.
- We develop a unified fractional Legendre spectral collocation scheme for the time-fractional Gray-Scott model, applicable to both one- and two-dimensional domains without requiring smoothing transformations, mesh grading, or auxiliary regularity treatments.
- All operational matrices are obtained in closed form, leading to a fully explicit algebraic discretization with high-order accuracy, even in the presence of intrinsic weak singularities associated with fractional dynamics.
- The proposed methodology establishes a new computational framework for nonlinear fractional reaction–diffusion systems, offering accuracy and generality not available in existing spectral approaches.

The remainder of the paper is organized as follows: Section 2 introduces one- and two-dimensional fractional-order shifted Legendre functions with some of their important properties. Section 3 presents the numerical technique for the one-dimensional time-fractional Gray-Scott model and derives two new one-dimensional FSLF-based operational matrices. Section 4 extends the application of the numerical scheme to the two-dimensional time-fractional Gray-Scott model. Section 5 tests the efficiency and accuracy of the presented numerical techniques by implementing two test problems and comparing the numerical resuls with other numerical techniques in the literature. Section 6 concludes the work.

2. Two-dimensional fractional-order Legendre functions

Recent developments on fractional Legendre-type bases and their operational structures have motivated the construction of the present scheme [28, 29]. These works provide key analytical tools that support the extensions introduced here and strengthen the theoretical framework underlying the proposed basis functions.

Throughout this section, the spatial variables satisfy

$$x \in [0, a], \qquad y \in [0, b], \qquad t \in [0, 1],$$

and the Legendre variable is defined by the standard mapping

$$z = \frac{2x}{a} - 1 \in [-1, 1].$$

Indices $i, j, k, m, l, n \in \mathbb{N}_0$ denote polynomial degrees, and the symbol α refers exclusively to the temporal truncation index used in the FSLF construction; it is unrelated to Jacobi parameters.

Let $P_j(z)$ denote the classical Legendre polynomial on $[-1, 1]$. The shifted Legendre polynomial (SLP) on $[0, a]$ is defined by

$$L_j^{(a)}(x) = P_j\left(\frac{2x}{a} - 1\right), \qquad x \in [0, a].$$

The SLP admits the power–series representation

$$L_j^{(a)}(x) = \sum_{m=0}^{j} \mathcal{E}_{j,m}^{(a)}\, x^m, \qquad \mathcal{E}_{j,m}^{(a)} = (-1)^{j-m} \frac{\Gamma(j+m+1)}{(j!)^2 (j-m)!\, a^m}. \tag{2.1}$$

These polynomials satisfy

$$\frac{d^s}{dx^s} L_j^{(a)}(0) = \chi_{j,s}^{(a)}, \qquad \chi_{j,s}^{(a)} = (-1)^{j-s} \frac{\Gamma(j+s+1)}{\Gamma(j-s+1)\Gamma(s+1) a^s},$$

$$\frac{d^s}{dx^s} L_j^{(a)}(a) = \psi_{j,s}^{(a)}, \qquad \psi_{j,s}^{(a)} = \frac{\Gamma(j+s+1)}{\Gamma(j-s+1)\Gamma(s+1) a^s}.$$

The SLPs satisfy the orthogonality relation

$$\int_0^a L_j^{(a)}(x)\, L_r^{(a)}(x)\, dx = \frac{a}{2r+1}\, \delta_{jr}. \tag{2.2}$$

Define the one-dimensional fractional shifted Legendre function (FSLF) by

$$\begin{cases} FL_{\mu,i,j}^{(a)}(t, x) = \displaystyle\sum_{l=0}^{i} \sum_{m=0}^{j} \mathcal{E}_{i,l}^{(1)}\, \mathcal{E}_{j,m}^{(a)}\, t^{l\mu} x^m, \qquad i, j \geq 0,\ 0 < \mu < 1, \\ FL_{\mu,i,j}^{(a)}(0, x) = \displaystyle\sum_{m=0}^{j} {}_L\mathfrak{X}_{i,0,j,m}^{(1,a)}\, x^m, \qquad {}_L\mathfrak{X}_{i,l,j,m}^{(a,b)} = \chi_{i,l}^{(a)}\, \mathcal{E}_{j,m}^{(b)}, \\ \dfrac{d^s}{dx^s} FL_{\mu,i,j}^{(a)}(t, 0) = \displaystyle\sum_{l=0}^{i} {}_L\mathfrak{X}_{j,s,i,l}^{(1,a)}\, t^{l\mu}, \\ \dfrac{d^s}{dx^s} FL_{\mu,i,j}^{(a)}(t, a) = \displaystyle\sum_{l=0}^{i} {}_R\mathfrak{X}_{j,s,i,l}^{(1,a)}\, t^{l\mu}, \qquad {}_R\mathfrak{X}_{i,l,j,m}^{(a,b)} = \psi_{i,l}^{(a)}\, \mathcal{E}_{j,m}^{(b)}. \end{cases} \tag{2.3}$$

The FSLFs satisfy the orthogonality condition

$$\int_0^1 \int_0^a FL_{\mu,i,j}^{(a)}(t, x)\, FL_{\mu,r,s}^{(a)}(t, x)\, t^{\mu-1}\, dx\, dt = \frac{a}{\mu(2r+1)(2s+1)}\, \delta_{ir}\delta_{js}. \tag{2.4}$$

Any function $g(t,x)$ square-integrable on $[0,1]\times[0,a]$ with respect to $t^{\mu-1}$ admits the expansion

$$\begin{cases} g_{\alpha,\beta}(t,x) = \mathcal{U}_{\alpha,\beta}^{T}\, F\mathfrak{Q}_{\alpha,\beta}^{\mu,a}(t,x), \\ \mathcal{U}_{\alpha,\beta} = [u_{0,0},\, u_{0,1},\ldots,u_{0,\beta},\; u_{1,0},\ldots,u_{\alpha,\beta}]^{T}, \\ F\mathfrak{Q}_{\alpha,\beta}^{\mu,a}(t,x) = [FL_{\mu,0,0}^{(a)},\ldots,FL_{\mu,0,\beta}^{(a)},FL_{\mu,1,0}^{(a)},\ldots,FL_{\mu,\alpha,\beta}^{(a)}]^{T}, \\ u_{i,j} = \dfrac{\mu(2i+1)(2j+1)}{a}\displaystyle\int_0^1\int_0^a g(t,x)\,FL_{\mu,i,j}^{(a)}(t,x)\,t^{\mu-1}\,dx\,dt. \end{cases} \tag{2.5}$$

We now extend (2.3) to two spatial dimensions by defining

$$\begin{cases} FL_{\mu,i,j,k}^{(a,b)}(t,x,y) = \displaystyle\sum_{l=0}^{i}\sum_{m=0}^{j}\sum_{n=0}^{k}\mathcal{E}_{i,l}^{(1)}\,\mathcal{E}_{j,m}^{(a)}\,\mathcal{E}_{k,n}^{(b)}\,t^{l\mu}x^{m}y^{n}, \\ FL_{\mu,i,j,k}^{(a,b)}(0,x,y) = \displaystyle\sum_{m=0}^{j}\sum_{n=0}^{k}{}_{L}\mathfrak{Y}_{i,0,j,m,k,n}^{(1,a,b)}\,x^{m}y^{n}, \\ \dfrac{d^{s}}{dx^{s}}FL_{\mu,i,j,k}^{(a,b)}(t,0,y) = \displaystyle\sum_{l=0}^{i}\sum_{n=0}^{k}{}_{L}\mathfrak{Y}_{j,s,i,l,k,n}^{(a,1,b)}\,t^{l\mu}y^{n}, \\ \dfrac{d^{s}}{dx^{s}}FL_{\mu,i,j,k}^{(a,b)}(t,a,y) = \displaystyle\sum_{l=0}^{i}\sum_{n=0}^{k}{}_{R}\mathfrak{Y}_{j,s,i,l,k,n}^{(a,1,b)}\,t^{l\mu}y^{n}, \\ \dfrac{d^{q}}{dy^{q}}FL_{\mu,i,j,k}^{(a,b)}(t,x,0) = \displaystyle\sum_{l=0}^{i}\sum_{m=0}^{j}{}_{L}\mathfrak{Y}_{k,q,i,l,j,m}^{(b,1,a)}\,t^{l\mu}x^{m}, \\ \dfrac{d^{q}}{dy^{q}}FL_{\mu,i,j,k}^{(a,b)}(t,x,b) = \displaystyle\sum_{l=0}^{i}\sum_{m=0}^{j}{}_{R}\mathfrak{Y}_{k,q,i,l,j,m}^{(b,1,a)}\,t^{l\mu}x^{m}. \end{cases} \tag{2.6}$$

These functions satisfy the orthogonality relation

$$\int_0^1\int_0^b\int_0^a FL_{\mu,i,j,k}^{(a,b)}(t,x,y)\,FL_{\mu,r,s,q}^{(a,b)}(t,x,y)\,t^{\mu-1}\,dx\,dy\,dt = \frac{ab}{(2r+1)(2s+1)(2q+1)}\delta_{ir}\delta_{js}\delta_{kq}. \tag{2.7}$$

Any function $g(t,x,y)$ square–integrable on $[0,1]\times[0,a]\times[0,b]$ with respect to $t^{\mu-1}$ admits the expansion

$$\begin{cases} g_{\alpha,\beta,\gamma}(t,x,y) = \mathcal{U}_{\alpha,\beta,\gamma}^{T}F\mathfrak{Q}_{\alpha,\beta,\gamma}^{\mu,a,b}(t,x,y), \\ F\mathfrak{Q}_{\alpha,\beta,\gamma}^{\mu,a,b}(t,x,y) = [FL_{\mu,0,0,0}^{(a,b)},\ldots,FL_{\mu,\alpha,\beta,\gamma}^{(a,b)}]^{T}, \\ u_{i,j,k} = \dfrac{\mu(2i+1)(2j+1)(2k+1)}{ab}\displaystyle\int_0^1\int_0^b\int_0^a g(t,x,y)\,FL_{\mu,i,j,k}^{(a,b)}(t,x,y)\,t^{\mu-1}\,dx\,dy\,dt. \end{cases} \tag{2.8}$$

3. The numerical scheme

This section is devoted to introducing a numerical method for solving the time-fractional Gray-Scott model:

$$\begin{aligned} {}_CD^{\mu}_{0,t}u(t,x) &= d_u\frac{\partial^2 u(t,x)}{\partial x^2} - u(t,x)v^2(t,x) + F(1-u(t,x)) + g_1(t,x),\\ {}_CD^{\mu}_{0,t}v(t,x) &= d_v\frac{\partial^2 v(t,x)}{\partial x^2} + u(t,x)v^2(t,x) - (F-K)v(t,x) + g_2(t,x), \end{aligned} \tag{3.1}$$

subjected to

$$\begin{aligned} &u(0,x) = \varrho_1(x), \quad u(t,0) = \epsilon_1(t), \quad u(t,a) = \delta_1(t),\\ &v(0,x) = \varrho_2(x), \quad v(t,0) = \epsilon_2(t), \quad v(t,a) = \delta_2(t), \end{aligned} \qquad 0 \le t \le 1,\ 0 \le x \le a, \tag{3.2}$$

where ${}_CD^{\mu}_{0,t}$ is the Caputo fractional-order derivative of order μ, for $0 < \mu \le 1$, and $g_r(t,x)$, $\mu_r(x)$, $\nu_r(t)$, and $\delta_r(t)$, with $r = 1, 2$, are known functions.

Lemma 1. *[30] For any integer $q \ge 0$, the shifted monomial $(z-1)^q$ can be expanded in the Legendre basis $\{P_m(z)\}_{m=0}^{q}$ as*

$$(z-1)^q = (-2)^q q! \sum_{m=0}^{q} \frac{(1+2m)\,(-q)_m}{(q+m+1)!}\, P_m(z), \qquad q \ge 0.$$

In other words, Lemma 1 provides the explicit Legendre-series representation of $(z-1)^q$ on $[-1,1]$ with known coefficients.

Theorem 1. *For any integer $q \ge 0$, the monomial x^q admits the shifted Legendre expansion*

$$\begin{aligned} x^q &= \sum_{m=0}^{q} S^{\,a}_{q,m}\, L_m^{(a)}(x),\\ S^{\,a}_{q,m} &= \sum_{n=0}^{q} \frac{(-1)^n a^q\,(-n)_m\,(1+2m)}{(q+1)_{-n}\,\Gamma(2+n+m)}, \end{aligned} \tag{3.3}$$

where the coefficients $S^{\,a}_{q,m}$ depend only on q, m, and the interval length a.

Equivalently, if we introduce the column vectors

$$\mathbf{X}_q(x) = [\,1,\ x,\ x^2,\ \ldots,\ x^q\,]^T, \qquad \mathbf{L}_q^{(a)}(x) = [\,L_0^{(a)}(x),\ L_1^{(a)}(x),\ \ldots,\ L_q^{(a)}(x)\,]^T,$$

then the expansion (3.3) *can be written in the compact matrix form*

$$\mathbf{X}_q(x) = \mathbf{S}_q^{(a)}\,\mathbf{L}_q^{(a)}(x),$$

where the $(q+1)\times(q+1)$ matrix $\mathbf{S}_q^{(a)} = (S^{\,a}_{p,m})_{0\le p,m\le q}$ collects the coefficients of all monomials x^p $(0 \le p \le q)$ in the shifted Legendre basis $\{L_m^{(a)}(x)\}_{m=0}^{q}$.

Proof. Setting $z = \frac{2x}{a} - 1$ in Lemma 1, and doing some lengthy manipulations, we get the desired result. □

Theorem 2. *For any integer $q \geq 0$ and $0 < \mu \leq 1$, the fractional monomial $x^{\mu q}$ can be expanded explicitly in the shifted Legendre basis evaluated at x^{μ} as*

$$x^{\mu q} = \sum_{m=0}^{q} S^{1}_{q,m} L^{(1)}_{m}(x^{\mu}),$$

where the coefficients $S^{1}_{q,m}$ are the same as those appearing in Theorem 1, given by

$$S^{1}_{q,m} = \sum_{n=0}^{q} \frac{(-1)^{n} (-n)_{m} (1 + 2m)}{(q+1)_{-n} \Gamma(2 + n + m)}.$$

This identity provides the explicit representation of $x^{\mu q}$ in terms of the polynomials $L^{(1)}_{m}(x^{\mu})$.

Proof. Applying a power of μ to the left side of Theorem 1, and doing some lengthy manipulations, gives the desired result. □

Theorem 3. *The second–order derivative of the vector $F\mathfrak{Q}^{\mu,a}_{\alpha,\beta}(t, x)$ can be written explicitly as*

$$\frac{\partial^2}{\partial x^2} F\mathfrak{Q}^{\mu,a}_{\alpha,\beta}(t, x) = \mathcal{S}^{x,2,a}_{\alpha,\beta} F\mathfrak{Q}^{\mu,a}_{\alpha,\beta}(t, x),$$

where the operational matrix of the second derivative is given by

$$\mathcal{S}^{x,2,a}_{\alpha,\beta} = \Phi_{\alpha} \otimes \Psi^{2,a}_{\beta}.$$

The matrix $\Phi_{\alpha} = (\phi_{i,r})_{0 \leq i,r \leq \alpha}$ contains the elements:

$$\phi_{i,r} = \sum_{l=0}^{i} \mathcal{E}^{(1)}_{i,l} S^{1}_{l,r}.$$

Similarly, the matrix $\Psi^{\zeta,a}_{\beta} = (\psi^{\zeta,a}_{j,s})_{0 \leq j,s \leq \beta}$ contains the elements:

$$\psi^{\zeta,a}_{j,s} = \sum_{m=\zeta}^{j} \frac{m!}{(m-\zeta)!} \mathcal{E}^{(a)}_{j,m} S^{a}_{m-\zeta,s}.$$

Proof. Taking the second-order derivative of the FSLF (2.3), we have

$$\begin{aligned} \frac{\partial^2}{\partial x^2} F J^{(a)}_{\mu,i,j}(t, x) &= \sum_{l=0}^{i} \sum_{m=0}^{j} \mathcal{E}^{(1)}_{i,l} \mathcal{E}^{(a)}_{j,m} t^{l\mu} \frac{\partial^2}{\partial x^2} x^{m} \\ &= \sum_{l=0}^{i} \sum_{m=2}^{j} \mathcal{E}^{(1)}_{i,l} \mathcal{E}^{(a)}_{j,m} m(m-1) t^{l\mu} x^{m-2}, \end{aligned}$$

and thanks to Theorems 1 and 2, we get

$$\frac{\partial^2}{\partial x^2} FL^{(a)}_{\mu,i,j}(t,x) = \sum_{l=0}^{i}\sum_{m=2}^{j} \mathcal{E}^{(1)}_{i,l}\mathcal{E}^{(a)}_{j,m} m(m-1)\left(\sum_{r=0}^{l}\sum_{s=0}^{m-2} S^{1}_{l,r} S^{a}_{m-2,s} L^{(1)}_{r}(t^{\mu}) L^{(a)}_{s}(x)\right),$$

which may be rewritten in the form

$$\begin{aligned}\frac{\partial^2}{\partial x^2} FL^{(a)}_{\mu,i,j}(t,x) &= \sum_{r=0}^{\alpha}\sum_{s=0}^{\beta}\left(\sum_{l=0}^{i}\sum_{m=2}^{j} m(m-1)\mathcal{E}^{(1)}_{i,l}\mathcal{E}^{(a)}_{j,m} S^{1}_{l,r} S^{a}_{m-2,s}\right) FL^{(a)}_{\mu,r,s}(t,x),\\ &= \sum_{r=0}^{\alpha}\sum_{s=0}^{\beta} \phi_{i,r}\psi^{\zeta,a}_{j,s} FL^{(a)}_{\mu,r,s}(t,x), \qquad 0 \le i \le \alpha,\ 0 \le j \le \beta,\end{aligned}$$

which completes the proof. □

Theorem 4. *The Caputo fractional derivative of order μ of the vector $F\mathfrak{Q}^{\mu,a}_{\alpha,\beta}(t,x)$ admits the explicit representation*

$$ {}_{C}D^{\mu}_{0,t} F\mathfrak{Q}^{\mu,a}_{\alpha,\beta}(t,x) = \mathcal{Q}^{\mu,a}_{\alpha,\beta} F\mathfrak{Q}^{\mu,a}_{\alpha,\beta}(t,x),$$

where the operational matrix of the Caputo derivative is given by

$$\mathcal{Q}^{\mu,a}_{\alpha,\beta} = \Theta^{\mu}_{\alpha} \otimes \Psi^{0,a}_{\beta}.$$

The matrix $\Theta^{\mu}_{\alpha} = (\theta^{\mu}_{i,q})_{0\le i,q\le\alpha}$ contains the temporal coefficients

$$\theta^{\mu}_{i,q} = \sum_{l=1}^{i} \frac{\Gamma(l\mu+1)}{\Gamma((l-1)\mu+1)} \mathcal{E}^{(1)}_{i,l} S^{1}_{l-1,q}.$$

Similarly, the matrix $\Psi^{0,a}_{\beta} = (\psi^{0,a}_{j,s})_{0\le j,s\le\beta}$ provides the expansion coefficients

$$\psi^{0,a}_{j,s} = \sum_{m=0}^{j} \mathcal{E}^{(a)}_{j,m} S^{a}_{m,s}.$$

Proof. Applying the Caputo fractional-order derivative of order μ of the FSLF (2.3), we have

$$\begin{aligned} {}_{C}D^{\mu}_{0,t} FL^{(a)}_{\mu,i,j}(t,x) &= \sum_{l=0}^{i}\sum_{m=0}^{j} \mathcal{E}^{(1)}_{i,l}\mathcal{E}^{(a)}_{j,m} x^{m} {}_{C}D^{\mu}_{0,t} t^{l\mu}\\ &= \sum_{l=1}^{i}\sum_{m=0}^{j} \mathcal{E}^{(1)}_{i,l}\mathcal{E}^{(a)}_{j,m} x^{m} \frac{\Gamma(l\mu+1)}{\Gamma((l-1)\mu+1)} t^{(l-1)\mu},\end{aligned}$$

and thanks to Theorems 1 and 2, we get

$$ {}_{C}D^{\mu}_{0,t} FL^{(a)}_{\mu,i,j}(t,x) = \sum_{l=1}^{i}\sum_{m=0}^{j} \mathcal{E}^{(1)}_{i,l}\mathcal{E}^{(a)}_{j,m} \frac{\Gamma(l\mu+1)}{\Gamma((l-1)\mu+1)}\left(\sum_{q=0}^{l-1}\sum_{s=0}^{m} S^{1}_{l-1,q} S^{a}_{m,s} L^{(1)}_{q}(t^{\mu}) L^{(a)}_{s}(x)\right),$$

which may be rewritten in the form

$$
\begin{aligned}
{}_C D^{\mu}_{0,t} F L^{(a)}_{\mu,i,j}(t,x) &= \sum_{q=0}^{\alpha}\sum_{s=0}^{\beta}\left(\sum_{l=1}^{i}\sum_{m=0}^{j}\frac{\Gamma(l\mu+1)}{\Gamma((l-1)\mu+1)}\mathcal{E}^{(1)}_{i,l}\mathcal{E}^{(a)}_{j,m}S^{1}_{l-1,q}S^{a}_{m,s}\right)FL^{(a)}_{\mu,q,s}(t,x),\\
&= \sum_{q=0}^{\alpha}\sum_{s=0}^{\beta}\theta^{\mu}_{i,q}\psi^{0,a}_{j,s}FL^{(a)}_{\mu,q,s}(t,x), \qquad 0\le i\le\alpha,\ 0\le j\le\beta.
\end{aligned}
$$

□

Now, the constructed numerical approach for (3.1) is to find $u_{\alpha,\beta}(t,x)$ and $v_{\alpha,\beta}(t,x)$, such that

$$
\begin{cases}
{}_C D^{\mu}_{0,t}u_{\alpha,\beta} = d_u\frac{\partial^2}{\partial x^2}u_{\alpha,\beta} - u_{\alpha,\beta}v^2_{\alpha,\beta} + F\left(1-u_{\alpha,\beta}\right) + g_1(t,x),\\
{}_C D^{\mu}_{0,t}v_{\alpha,\beta} = d_v\frac{\partial^2}{\partial x^2}v_{\alpha,\beta} + u_{\alpha,\beta}v^2_{\alpha,\beta} - (F-K)v_{\alpha,\beta} + g_2(t,x),\\
u_{\alpha,\beta}(0,x) = \varrho_1(x), \qquad u_{\alpha,\beta}(t,0) = \epsilon_1(t), \qquad u_{\alpha,\beta}(t,a) = \delta_1(t),\\
v_{\alpha,\beta}(0,x) = \varrho_2(x), \qquad v_{\alpha,\beta}(t,0) = \epsilon_2(t), \qquad v_{\alpha,\beta}(t,a) = \delta_2(t).
\end{cases}
\tag{3.4}
$$

Let

$$
\begin{aligned}
u_{\alpha,\beta}(t,x) &= \mathcal{U}^T_{\alpha,\beta}F\mathfrak{L}^{\mu,a}_{\alpha,\beta}(t,x), \qquad & \mathcal{U}_{\alpha,\beta} &= \left[u_{0,0},\ \cdots,\ u_{\alpha,\beta}\right]^T,\\
v_{\alpha,\beta}(t,x) &= \mathcal{V}^T_{\alpha,\beta}F\mathfrak{L}^{\mu,a}_{\alpha,\beta}(t,x), \qquad & \mathcal{V}_{\alpha,\beta} &= \left[v_{0,0},\ \cdots,\ v_{\alpha,\beta}\right]^T,
\end{aligned}
\tag{3.5}
$$

which leads to

$$
\begin{aligned}
{}_C D^{\mu}_{0,t}u_{\alpha,\beta}(t,x) &= \mathcal{U}^T_{\alpha,\beta C}D^{\mu}_{0,t}F\mathfrak{L}^{\mu,a}_{\alpha,\beta}(t,x), \qquad & \frac{\partial^2}{\partial x^2}u_{\alpha,\beta}(t,x) &= \mathcal{U}^T_{\alpha,\beta}\frac{\partial^2}{\partial x^2}F\mathfrak{L}^{\mu,a}_{\alpha,\beta}(t,x),\\
{}_C D^{\mu}_{0,t}v_{\alpha,\beta}(t,x) &= \mathcal{V}^T_{\alpha,\beta C}D^{\mu}_{0,t}F\mathfrak{L}^{\mu,a}_{\alpha,\beta}(t,x), \qquad & \frac{\partial^2}{\partial x^2}v_{\alpha,\beta}(t,x) &= \mathcal{V}^T_{\alpha,\beta}\frac{\partial^2}{\partial x^2}F\mathfrak{L}^{\mu,a}_{\alpha,\beta}(t,x).
\end{aligned}
$$

Thanks to Theorems 3 and 4, one can write

$$
\begin{aligned}
{}_C D^{\mu}_{0,t}u_{\alpha,\beta}(t,x) &= \mathcal{U}^T_{\alpha,\beta}\mathcal{Q}^{\mu,a}_{\alpha,\beta}F\mathfrak{L}^{\mu,a}_{\alpha,\beta}(t,x), \qquad & \frac{\partial^2}{\partial x^2}u_{\alpha,\beta}(t,x) &= \mathcal{U}^T_{\alpha,\beta}\mathcal{S}^{x,2,a}_{\alpha,\beta}F\mathfrak{L}^{\mu,a}_{\alpha,\beta}(t,x),\\
{}_C D^{\mu}_{0,t}v_{\alpha,\beta}(t,x) &= \mathcal{V}^T_{\alpha,\beta}\mathcal{Q}^{\mu,a}_{\alpha,\beta}F\mathfrak{L}^{\mu,a}_{\alpha,\beta}(t,x), \qquad & \frac{\partial^2}{\partial x^2}v_{\alpha,\beta}(t,x) &= \mathcal{V}^T_{\alpha,\beta}\mathcal{S}^{x,2,a}_{\alpha,\beta}F\mathfrak{L}^{\mu,a}_{\alpha,\beta}(t,x).
\end{aligned}
$$

Then, one can write the residual of (3.4) as follows:

$$
\begin{aligned}
{}^1\mathcal{R}_{\alpha,\beta}(t,x) &= \mathcal{U}^T_{\alpha,\beta}\mathcal{Q}^{\mu,a}_{\alpha,\beta}F\mathfrak{L}^{\mu,a}_{\alpha,\beta}(t,x) + \left(\mathcal{U}^T_{\alpha,\beta}F\mathfrak{L}^{\mu,a}_{\alpha,\beta}(t,x)\right)\left(\mathcal{V}^T_{\alpha,\beta}F\mathfrak{L}^{\mu,a}_{\alpha,\beta}(t,x)\right)^2\\
&\quad - d_u\mathcal{U}^T_{\alpha,\beta}\mathcal{S}^{x,2,a}_{\alpha,\beta}F\mathfrak{L}^{\mu,a}_{\alpha,\beta}(t,x) - F(1-\mathcal{U}^T_{\alpha,\beta}F\mathfrak{L}^{\mu,a}_{\alpha,\beta}(t,x)) - g_1(t,x),\\
{}^2\mathcal{R}_{\alpha,\beta}(t,x) &= \mathcal{V}^T_{\alpha,\beta}\mathcal{Q}^{\mu,a}_{\alpha,\beta}F\mathfrak{L}^{\mu,a}_{\alpha,\beta}(t,x) - \left(\mathcal{U}^T_{\alpha,\beta}F\mathfrak{L}^{\mu,a}_{\alpha,\beta}(t,x)\right)\left(\mathcal{V}^T_{\alpha,\beta}F\mathfrak{L}^{\mu,a}_{\alpha,\beta}(t,x)\right)^2\\
&\quad - d_v\mathcal{V}^T_{\alpha,\beta}\mathcal{S}^{x,2,a}_{\alpha,\beta}F\mathfrak{L}^{\mu,a}_{\alpha,\beta}(t,x) + (F-K)\mathcal{V}^T_{\alpha,\beta}F\mathfrak{L}^{\mu,a}_{\alpha,\beta}(t,x) - g_2(t,x).
\end{aligned}
$$

Collocating the above system as $(t_{\mu,\rho}, x_{a,\upsilon})$, the roots of FSLF $F\mathfrak{L}^{(a)}_{\mu,\alpha+1,\beta+1}(t,x)$, generates a system of $2(\alpha+1)(\beta+1)$ algebraic equations as follows:

$$
\begin{aligned}
{}^1\mathcal{R}_{\alpha,\beta}(t_{\mu,\rho},x_{a,\upsilon}) &= 0, \qquad & 1\le\rho\le\alpha,\ 1\le\upsilon\le\beta-1,\\
{}^2\mathcal{R}_{\alpha,\beta}(t_{\mu,\rho},x_{a,\upsilon}) &= 0, \qquad & 1\le\rho\le\alpha,\ 1\le\upsilon\le\beta-1,
\end{aligned}
\tag{3.6}
$$

$$\begin{aligned}
&\mathcal{U}^T_{\alpha,\beta} F\mathfrak{Q}^{\mu,a}_{\alpha,\beta}(0, x_{a,\upsilon}) = \varrho_1(x_{a,\upsilon}), \qquad 0 \le \upsilon \le \beta,\\
&\mathcal{V}^T_{\alpha,\beta} F\mathfrak{Q}^{\mu,a}_{\alpha,\beta}(0, x_{a,\upsilon}) = \varrho_2(x_{a,\upsilon}), \qquad 0 \le \upsilon \le \beta,
\end{aligned} \tag{3.7}$$

$$\begin{aligned}
&\mathcal{U}^T_{\alpha,\beta} F\mathfrak{Q}^{\mu,a}_{\alpha,\beta}(t_{\mu,\rho}, 0) = \epsilon_1(t_{\mu,\rho}), \qquad 1 \le \rho \le \alpha,\\
&\mathcal{V}^T_{\alpha,\beta} F\mathfrak{Q}^{\mu,a}_{\alpha,\beta}(t_{\mu,\rho}, 0) = \epsilon_2(t_{\mu,\rho}), \qquad 1 \le \rho \le \alpha,\\
&\mathcal{U}^T_{\alpha,\beta} F\mathfrak{Q}^{\mu,a}_{\alpha,\beta}(t_{\mu,\rho}, a) = \delta_1(t_{\mu,\rho}), \qquad 1 \le \rho \le \alpha,\\
&\mathcal{V}^T_{\alpha,\beta} F\mathfrak{Q}^{\mu,a}_{\alpha,\beta}(t_{\mu,\rho}, a) = \delta_2(t_{\mu,\rho}), \qquad 1 \le \rho \le \alpha.
\end{aligned} \tag{3.8}$$

Finally, an appropriate numerical method is employed to solve system (3.6)–(3.8), yielding the unknowns $u_{i,j},\ v_{i,j}$ $(0 \le i \le \alpha,\ 0 \le j \le \beta)$, and consequently getting the numerical solution (3.5). The essential computational steps of the proposed collocation formulation are summarized in Algorithm 1, which provide a clear procedural outline of the implementation.

Algorithm 1: One-dimensional FSLF collocation scheme

Step 1	Fix $0 < \mu \le 1$, d_u, d_v, F, K, domain length a, and truncation indices α, β.
Step 2	Construct the 1D FSLF basis $F\mathfrak{Q}^{\mu,a}_{\alpha,\beta}(t, x)$ using (2.3)–(2.5).
Step 3	Assemble the operational matrices $\mathcal{S}^{x,2,a}_{\alpha,\beta}$ and $\mathcal{Q}^{\mu,a}_{\alpha,\beta}$ from Theorems 3 and 4.
Step 4	Choose collocation nodes $(t_{\mu,\rho}, x_{a,\upsilon})$ as the roots of $F\mathfrak{Q}^{\mu,a}_{\alpha+1,\beta+1}(t, x)$ and add boundary points.
Step 5	Express $u_{\alpha,\beta}, v_{\alpha,\beta}$ as in (3.5), form the residuals ${}^1\mathcal{R}_{\alpha,\beta}$, ${}^2\mathcal{R}_{\alpha,\beta}$, collocate them, and impose (3.2) to obtain the algebraic system (3.6).
Step 6	Solve (3.6) for $\mathcal{U}_{\alpha,\beta}$ and $\mathcal{V}_{\alpha,\beta}$ and reconstruct $u_{\alpha,\beta}(t, x)$, $v_{\alpha,\beta}(t, x)$ via (3.5).

4. Two-dimensional case

In this section, we study the application of the numerical scheme to the time-fractional Gray-Scott model in two dimensions. We consider

$$\begin{aligned}
{}_CD^{\mu}_{0,t} u(t, x, y) &= d_u \frac{\partial^2 u(t, x, y)}{\partial x^2} + d_u \frac{\partial^2 u(t, x, y)}{\partial y^2} - u(t, x, y)v^2(t, x, y) + F(1 - u(t, x, y)) + g_1(t, x, y),\\
{}_CD^{\mu}_{0,t} v(t, x, y) &= d_v \frac{\partial^2 v(t, x, y)}{\partial x^2} + d_v \frac{\partial^2 v(t, x, y)}{\partial y^2} + u(t, x, y)v^2(t, x, y) - (F - K)v(t, x, y) + g_2(t, x, y),
\end{aligned} \tag{4.1}$$

subjected to

$$\begin{aligned}
&u(0, x, y) = \varrho_1(x, y), \qquad v(0, x, y) = \varrho_2(x, y),\\
&u(t, 0, y) = \epsilon_1(t, y), \qquad v(t, 0, y) = \epsilon_2(t, y),\\
&u(t, a, y) = \delta_1(t, y), \qquad v(t, a, y) = \delta_2(t, y),\\
&u(t, x, 0) = \nu_1(t, x), \qquad v(t, x, 0) = \nu_2(t, x),\\
&u(t, a, y) = \sigma_1(t, x), \qquad v(t, a, y) = \sigma_2(t, x),
\end{aligned} \tag{4.2}$$

where $g_r(t, x, y)$, $\mu_r(x, y)$, $\nu_r(t, y)$, $\delta_r(t, y)$, $\epsilon_r(t, x)$, and $\varrho_r(t, x)$, with $r = 1, 2$, are known functions. We begin by deriving three theorems that play an important role in what follows.

Theorem 5. *The second-order derivative in x of the two-dimensional vector satisfies*

$$\frac{\partial^2}{\partial x^2} F\mathfrak{Q}^{\mu,a,b}_{\alpha,\beta,\gamma}(t,x,y) = \mathcal{S}^{x,2,a,b}_{\alpha,\beta,\gamma} F\mathfrak{Q}^{\mu,a}_{\alpha,\beta,\gamma}(t,x,y); \qquad \mathcal{S}^{x,2,a,b}_{\alpha,\beta,\gamma} = \Phi_\alpha \otimes \Psi^{2,a}_\beta \otimes \Psi^{0,b}_\gamma.$$

Proof. Taking the second-order derivative of the two-dimensional FSLF (2.6) w.r.t. x, we have

$$\begin{aligned}\frac{\partial^2}{\partial x^2} FL^{(a,b)}_{\mu,i,j,k}(t,x,y) &= \sum_{l=0}^{i}\sum_{m=0}^{j}\sum_{n=0}^{k} \mathcal{E}^{(1)}_{i,l}\mathcal{E}^{(a)}_{j,m}\mathcal{E}^{(b)}_{k,n}\, t^{l\mu} y^n \frac{\partial^2}{\partial x^2} x^m \\ &= \sum_{l=0}^{i}\sum_{m=2}^{j}\sum_{n=0}^{k} \mathcal{E}^{(1)}_{i,l}\mathcal{E}^{(a)}_{j,m,j}\mathcal{E}^{(b)}_{k,n}\, t^{l\mu} y^n m(m-1)x^{m-2},\end{aligned}$$

and thanks to Theorems 1 and 2, we get

$$\frac{\partial^2}{\partial x^2} FL^{(a,b)}_{\mu,i,j,k}(t,x,y) = \sum_{l=0}^{i}\sum_{m=2}^{j}\sum_{n=0}^{k} \mathcal{E}^{(1)}_{i,j}\mathcal{E}^{(a)}_{j,m}\mathcal{E}^{(b)}_{k,n} m(m-1) \times \left(\sum_{r=0}^{l}\sum_{s=0}^{m-2}\sum_{q=0}^{n} S^{1}_{l,r} S^{a}_{m-2,s} S^{b}_{n,q} J^{(1)}_r(t^\mu) L^{(a)}_s(x) L^{(b)}_q(y) \right),$$

which may be rewritten in the form

$$\frac{\partial^2}{\partial x^2} FL^{(a,b)}_{\mu,i,j,k}(t,x,y) = \sum_{r=0}^{\alpha}\sum_{s=0}^{\beta}\sum_{q=0}^{\gamma} \phi_{i,r}\psi^{2,a}_{j,s}\psi^{0,b}_{k,q} FL^{(a,b)}_{\mu,r,s,q}(t,x,y),$$

and this completes the proof. □

Theorem 6. *The second–order derivative in y of the two–dimensional vector satisfies*

$$\frac{\partial^2}{\partial y^2} F\mathfrak{Q}^{\lambda,a,b}_{\alpha,\beta,\gamma}(t,x,y) = \mathcal{S}^{y,2,a,b}_{\alpha,\beta,\gamma}\, F\mathfrak{Q}^{\lambda,a,b}_{\alpha,\beta,\gamma}(t,x,y),$$

where

$$\mathcal{S}^{y,2,a,b}_{\alpha,\beta,\gamma} = \Phi_\alpha \otimes \Psi^{0,a}_\beta \otimes \Psi^{2,b}_\gamma.$$

Proof. Taking the second-order derivative of the two-dimensional FSLF (2.6) w.r.t. y, we have

$$\begin{aligned}\frac{\partial^2}{\partial y^2} FL^{(a,b)}_{\mu,i,j,k}(t,x,y) &= \sum_{l=0}^{i}\sum_{m=0}^{j}\sum_{n=0}^{k} \mathcal{E}^{(1)}_{i,l}\mathcal{E}^{(a)}_{j,m}\mathcal{E}^{(b)}_{k,n}\, t^{l\mu} x^m \frac{\partial^2}{\partial y^2} y^n \\ &= \sum_{l=0}^{i}\sum_{m=0}^{j}\sum_{n=2}^{k} \mathcal{E}^{(1)}_{i,l}\mathcal{E}^{(a)}_{j,m}\mathcal{E}^{(b)}_{k,n}\, t^{l\mu} x^m n(n-1) y^{n-2} \\ &= \sum_{l=0}^{i}\sum_{m=0}^{j}\sum_{n=2}^{k} \mathcal{E}^{(1)}_{i,l}\mathcal{E}^{(a)}_{j,m}\mathcal{E}^{(b)}_{k,n} n(n-1) \\ &\quad \times \left(\sum_{r=0}^{l}\sum_{s=0}^{m}\sum_{q=0}^{n-2} S^{1}_{l,r} S^{a}_{m,s} S^{b}_{n-2,q} L^{(1)}_r(t^\mu) L^{(a)}_s(x) L^{(b)}_q(y) \right) \\ &= \sum_{r=0}^{\alpha}\sum_{s=0}^{\beta}\sum_{q=0}^{\gamma} \phi_{i,r}\psi^{0,a}_{j,s}\psi^{2,b}_{k,q} FL^{(a,b)}_{\mu,r,s,q}(t,x,y).\end{aligned}$$

□

Theorem 7. *The Caputo fractional derivative of order μ of the two-dimensional vector satisfies*

$$ {}_{C}D^{\mu}_{0,t} F\mathfrak{L}^{\mu,a,b}_{\alpha,\beta,\gamma}(t,x,y) = \mathcal{Q}^{\mu,a,b}_{\alpha,\beta,\gamma}\, F\mathfrak{L}^{\mu,a,b}_{\alpha,\beta,\gamma}(t,x,y), $$

where

$$ \mathcal{Q}^{\mu,a,b}_{\alpha,\beta,\gamma} = \Theta^{\mu}_{\alpha} \otimes \Psi^{0,a}_{\beta} \otimes \Psi^{0,b}_{\gamma}. $$

The matrices are defined by

$$ \theta^{\mu}_{i,q} = \sum_{l=1}^{i} \frac{\Gamma(l\mu+1)}{\Gamma((l-1)\mu+1)} \mathcal{E}^{(1)}_{i,l}\, S^{1}_{l-1,q}, $$

and

$$ \psi^{0,a}_{j,s} = \sum_{m=0}^{j} \mathcal{E}^{(a)}_{j,m}\, S^{a}_{m,s}, \qquad \psi^{0,b}_{k,q} = \sum_{n=0}^{k} \mathcal{E}^{(b)}_{k,n}\, S^{b}_{n,q}. $$

Proof. Applying the Caputo fractional-order derivative of order μ of the two-dimensional FSLF (2.6) w.r.t. t, we have

$$ \begin{aligned} {}_{C}D^{\mu}_{0,t} FL^{(a,b)}_{\mu,i,j,k}(t,x,y) &= \sum_{l=0}^{i}\sum_{m=0}^{j}\sum_{n=0}^{k} \mathcal{E}^{(1)}_{i,l}\mathcal{E}^{(a)}_{j,m}\mathcal{E}^{(b)}_{k,n}\, x^{m}y^{n}\, {}_{C}D^{\mu}_{0,t} t^{l\mu} \\ &= \sum_{l=1}^{i}\sum_{m=0}^{j}\sum_{n=0}^{k} \mathcal{E}^{(1)}_{i,l}\mathcal{E}^{(a)}_{j,m}\mathcal{E}^{(b)}_{k,n}\, x^{m}y^{n} \frac{\Gamma(l\mu+1)}{\Gamma((l-1)\mu+1)} t^{(l-1)\mu} \\ &= \sum_{l=1}^{i}\sum_{m=0}^{j}\sum_{n=0}^{k} \mathcal{E}^{(1)}_{i,l}\mathcal{E}^{(a)}_{j,m}\mathcal{E}^{(b)}_{k,n} \frac{\Gamma(l\mu+1)}{\Gamma((l-1)\mu+1)} \\ &\quad \times \left(\sum_{q=0}^{l-1}\sum_{s=0}^{m}\sum_{z=0}^{k} S^{1}_{p,q} S^{a}_{m,s} S^{a}_{k,z} L^{(1)}_{q}(t^{\mu}) L^{(a)}_{s}(x) L^{(b)}_{z}(y) \right) \\ &= \sum_{q=0}^{\alpha}\sum_{s=0}^{\beta}\sum_{z=0}^{\gamma} \theta^{\mu}_{i,q}\psi^{0,a}_{j,s}\psi^{0,b}_{k,z} FL^{(a,b)}_{\mu,q,s,z}(t,x,y). \end{aligned} $$

□

Now, we expand the functions $u(t,x,y)$ and $v(t,x,y)$ in terms of the two-dimensional FSLF as follows:

$$ \begin{aligned} u_{\alpha,\beta,\gamma}(t,x,y) &= \mathcal{U}^{T}_{\alpha,\beta,\gamma} F\mathfrak{L}^{\mu,a,b}_{\alpha,\beta,\gamma}(t,x,y), & \mathcal{U}_{\alpha,\beta,\gamma} &= \left[u_{0,0,0},\ \cdots,\ u_{\alpha,\beta,\gamma}\right]^{T}, \\ v_{\alpha,\beta,\gamma}(t,x,y) &= \mathcal{V}^{T}_{\alpha,\beta,\gamma} F\mathfrak{L}^{\mu,a,b}_{\alpha,\beta,\gamma}(t,x,y), & \mathcal{V}_{\alpha,\beta,\gamma} &= \left[v_{0,0,0},\ \cdots,\ v_{\alpha,\beta,\gamma}\right]^{T}. \end{aligned} \tag{4.3} $$

Then, thanks to Theorem 5, we have

$$ \begin{aligned} {}_{C}D^{\mu}_{0,t} u_{\alpha,\beta,\gamma}(t,x,y) &= \mathcal{U}^{T}_{\alpha,\beta,\gamma\,C}D^{\mu}_{0,t} F\mathfrak{L}^{\mu,a,b}_{\alpha,\beta,\gamma}(t,x,y) = \mathcal{U}^{T}_{\alpha,\beta,\gamma}\mathcal{Q}^{\mu,a,b}_{\alpha,\beta,\gamma} F\mathfrak{L}^{\mu,a,b}_{\alpha,\beta,\gamma}(t,x,y), \\ {}_{C}D^{\mu}_{0,t} v_{\alpha,\beta,\gamma}(t,x,y) &= \mathcal{V}^{T}_{\alpha,\beta,\gamma\,C}D^{\mu}_{0,t} F\mathfrak{L}^{\mu,a,b}_{\alpha,\beta,\gamma}(t,x,y) = \mathcal{V}^{T}_{\alpha,\beta,\gamma}\mathcal{Q}^{\mu,a,b}_{\alpha,\beta,\gamma} F\mathfrak{L}^{\mu,a,b}_{\alpha,\beta,\gamma}(t,x,y). \end{aligned} \tag{4.4} $$

Theorem 6 gives

$$\begin{aligned}\frac{\partial^2}{\partial x^2}u_{\alpha,\beta,\gamma}(t,x,y) &= \mathcal{U}^T_{\alpha,\beta,\gamma}\frac{\partial^2}{\partial x^2}F\mathfrak{Q}^{\mu,a,b}_{\alpha,\beta,\gamma}(t,x,y) = \mathcal{U}^T_{\alpha,\beta,\gamma}\mathcal{S}^{x,2,a,b}_{\alpha,\beta,\gamma}F\mathfrak{Q}^{\mu,a,b}_{\alpha,\beta,\gamma}(t,x,y),\\ \frac{\partial^2}{\partial x^2}v_{\alpha,\beta,\gamma}(t,x,y) &= \mathcal{V}^T_{\alpha,\beta,\gamma}\frac{\partial^2}{\partial x^2}F\mathfrak{Q}^{\mu,a,b}_{\alpha,\beta,\gamma}(t,x,y) = \mathcal{V}^T_{\alpha,\beta,\gamma}\mathcal{S}^{x,2,a,b}_{\alpha,\beta,\gamma}F\mathfrak{Q}^{\mu,a,b}_{\alpha,\beta,\gamma}(t,x,y).\end{aligned} \tag{4.5}$$

Also Theorem 7 gives

$$\begin{aligned}\frac{\partial^2}{\partial y^2}u_{\alpha,\beta,\gamma}(t,x,y) &= \mathcal{U}^T_{\alpha,\beta,\gamma}\frac{\partial^2}{\partial y^2}F\mathfrak{Q}^{\mu,a,b}_{\alpha,\beta,\gamma}(t,x,y) = \mathcal{U}^T_{\alpha,\beta,\gamma}\mathcal{S}^{y,2,a,b}_{\alpha,\beta,\gamma}F\mathfrak{Q}^{\mu,a,b}_{\alpha,\beta,\gamma}(t,x,y),\\ \frac{\partial^2}{\partial y^2}v_{\alpha,\beta,\gamma}(t,x,y) &= \mathcal{V}^T_{\alpha,\beta,\gamma}\frac{\partial^2}{\partial y^2}F\mathfrak{Q}^{\mu,a,b}_{\alpha,\beta,\gamma}(t,x,y) = \mathcal{V}^T_{\alpha,\beta,\gamma}\mathcal{S}^{y,2,a,b}_{\alpha,\beta,\gamma}F\mathfrak{Q}^{\mu,a,b}_{\alpha,\beta,\gamma}(t,x,y).\end{aligned} \tag{4.6}$$

The spectral collocation approach is to find $u_{\alpha,\beta,\gamma}(t,x,y)$ and $v_{\alpha,\beta,\gamma}(t,x,y)$, such that

$$\begin{aligned}{}_cD^{\mu}_{0,t}u_{\alpha,\beta,\gamma} &= d_u\frac{\partial^2}{\partial x^2}u_{\alpha,\beta,\gamma} + d_u\frac{\partial^2}{\partial y^2}u_{\alpha,\beta,\gamma} - u_{\alpha,\beta,\gamma}v^2_{\alpha,\beta,\gamma} + F(1-u_{\alpha,\beta,\gamma}) + g_1(t,x,y),\\ {}_cD^{\mu}_{0,t}v_{\alpha,\beta,\gamma} &= d_v\frac{\partial^2}{\partial x^2}v_{\alpha,\beta,\gamma} + d_v\frac{\partial^2}{\partial y^2}v_{\alpha,\beta,\gamma} + u_{\alpha,\beta,\gamma}v^2_{\alpha,\beta,\gamma} - (F-K)v_{\alpha,\beta,\gamma} + g_2(t,x,y),\end{aligned} \tag{4.7}$$

and

$$\begin{aligned}&u_{\alpha,\beta,\gamma}(0,x,y) = \varrho_1(x,y), \quad && v_{\alpha,\beta,\gamma}(0,x,y) = \varrho_2(x,y),\\ &u_{\alpha,\beta,\gamma}(t,0,y) = \epsilon_1(t,y), && v_{\alpha,\beta,\gamma}(t,0,y) = \epsilon_2(t,y),\\ &u_{\alpha,\beta,\gamma}(t,a,y) = \delta_1(t,y), && v_{\alpha,\beta,\gamma}(t,a,y) = \delta_2(t,y),\\ &u_{\alpha,\beta,\gamma}(t,x,0) = \nu_1(t,x), && v_{\alpha,\beta,\gamma}(t,x,0) = \nu_2(t,x),\\ &u_{\alpha,\beta,\gamma}(t,a,y) = \sigma_1(t,x), && v_{\alpha,\beta,\gamma}(t,a,y) = \sigma_2(t,x).\end{aligned} \tag{4.8}$$

Then, one can write the residual of (4.7) as follows:

$$\begin{aligned}{}^1\mathcal{R}_{\alpha,\beta,\gamma}(t,x,y) &= \mathcal{U}^T_{\alpha,\beta,\gamma}\mathcal{Q}^{\mu,a,b}_{\alpha,\beta,\gamma}F\mathfrak{Q}^{\mu,a,b}_{\alpha,\beta,\gamma}(t,x,y) - F\left(1-\mathcal{U}^T_{\alpha,\beta,\gamma}F\mathfrak{Q}^{\mu,a,b}_{\alpha,\beta,\gamma}(t,x,y)\right)\\ &\quad - d_u\mathcal{U}^T_{\alpha,\beta,\gamma}\mathcal{S}^{x,2,a,b}_{\alpha,\beta,\gamma}F\mathfrak{Q}^{\sigma_1,a}_{\alpha,\beta,\gamma}(t,x,y) - d_u\mathcal{U}^T_{\alpha,\beta,\gamma}\mathcal{S}^{y,2,a,b}_{\alpha,\beta,\gamma}F\mathfrak{Q}^{\mu,a}_{\alpha,\beta,\gamma}(t,x,y)\\ &\quad + \left(\mathcal{U}^T_{\alpha,\beta,\gamma}F\mathfrak{Q}^{\mu,a,b}_{\alpha,\beta,\gamma}(t,x,y)\right)\left(\mathcal{V}^T_{\alpha,\beta,\gamma}F\mathfrak{Q}^{\mu,a,b}_{\alpha,\beta,\gamma}(t,x,y)\right)^2 - g_1(t,x,y),\\ {}^2\mathcal{R}_{\alpha,\beta,\gamma}(t,x,y) &= \mathcal{V}^T_{\alpha,\beta,\gamma}\mathcal{Q}^{\mu,a,b}_{\alpha,\beta,\gamma}F\mathfrak{Q}^{\sigma_2,a,b}_{\alpha,\beta,\gamma}(t,x,y) + (F-K)\mathcal{V}^T_{\alpha,\beta,\gamma}F\mathfrak{Q}^{\mu,a,b}_{\alpha,\beta,\gamma}(t,x,y)\\ &\quad - d_v\mathcal{V}^T_{\alpha,\beta,\gamma}\mathcal{S}^{x,2,a,b}_{\alpha,\beta,\gamma}F\mathfrak{Q}^{\mu,a,b}_{\alpha,\beta,\gamma}(t,x,y) - d_v\mathcal{V}^T_{\alpha,\beta,\gamma}\mathcal{S}^{y,2,a,b}_{\alpha,\beta,\gamma}F\mathfrak{Q}^{\mu,a,b}_{\alpha,\beta,\gamma}(t,x,y)\\ &\quad + \left(\mathcal{U}^T_{\alpha,\beta,\gamma}F\mathfrak{Q}^{\mu,a,b}_{\alpha,\beta,\gamma}(t,x,y)\right)\left(\mathcal{V}^T_{\alpha,\beta,\gamma}F\mathfrak{Q}^{\mu,a,b}_{\alpha,\beta,\gamma}(t,x,y)\right)^2 - g_2(t,x,y).\end{aligned}$$

To proceed, we now construct a system of $2\alpha(\beta-1)(\gamma-1)$ algebraic equations by collocating the residuals as follows:

$$\begin{aligned}{}^1\mathcal{R}_{\alpha,\beta,\gamma}(t_{\mu,\rho},x_{a,\upsilon},y_{b,\tau}) &= 0, \qquad 1\le\rho\le\alpha,\ 1\le\upsilon\le\beta-1,\ 1\le\tau\le\gamma-1,\\ {}^2\mathcal{R}_{\alpha,\beta,\gamma}(t_{\mu,\rho},x_{a,\upsilon},y_{b,\tau}) &= 0, \qquad 1\le\rho\le\alpha,\ 1\le\upsilon\le\beta-1,\ 1\le\tau\le\gamma-1,\end{aligned} \tag{4.9}$$

with the following system of $2(\beta+1)(\gamma+1)+4\alpha(\gamma+1)+4\alpha\beta$ algebraic equations:

$$\begin{aligned}
&\mathcal{U}^{T}_{\alpha,\beta,\gamma}F\mathfrak{L}^{\mu,a,b}_{\alpha,\beta,\gamma}(0,x_{a,\upsilon},y_{b,\tau})=\varrho_1(x_{a,\upsilon},y_{b,\tau}), && 0\le\upsilon\le\beta,\quad 0\le\tau\le\gamma,\\
&\mathcal{V}^{T}_{\alpha,\beta,\gamma}F\mathfrak{L}^{\mu,a,b}_{\alpha,\beta,\gamma}(0,x_{a,\upsilon},y_{b,\tau})=\varrho_2(x_{a,\upsilon},y_{b,\tau}), && 0\le\upsilon\le\beta,\quad 0\le\tau\le\gamma,\\
&\mathcal{U}^{T}_{\alpha,\beta,\gamma}F\mathfrak{L}^{\mu,a,b}_{\alpha,\beta,\gamma}(t_{\mu,\rho},0,y_{b,\tau})=\epsilon_1(t_{\mu,\rho},y_{b,\tau}), && 1\le\rho\le\alpha,\quad 0\le\tau\le\gamma,\\
&\mathcal{V}^{T}_{\alpha,\beta,\gamma}F\mathfrak{L}^{\mu,a,b}_{\alpha,\beta,\gamma}(t_{\mu,\rho},0,y_{b,\tau})=\epsilon_2(t_{\mu,\rho},y_{b,\tau}), && 1\le\rho\le\alpha,\quad 0\le\tau\le\gamma,\\
&\mathcal{U}^{T}_{\alpha,\beta,\gamma}F\mathfrak{L}^{\mu,a,b}_{\alpha,\beta,\gamma}(t_{\mu,\rho},a,y_{b,\tau})=\delta_1(t_{\mu,\rho},y_{b,\tau}), && 1\le\rho\le\alpha,\quad 0\le\tau\le\gamma,\\
&\mathcal{V}^{T}_{\alpha,\beta,\gamma}F\mathfrak{L}^{\mu,a,b}_{\alpha,\beta,\gamma}(t_{\mu,\rho},a,y_{b,\tau})=\delta_2(t_{\mu,\rho},y_{b,\tau}), && 1\le\rho\le\alpha,\quad 0\le\tau\le\gamma,\\
&\mathcal{U}^{T}_{\alpha,\beta,\gamma}F\mathfrak{L}^{\mu,a,b}_{\alpha,\beta,\gamma}(t_{\mu,\rho},x_{a,\upsilon},0)=\nu_1(t_{\mu,\rho},x_{a,\upsilon}), && 1\le\rho\le\alpha,\quad 1\le\upsilon\le\beta-1,\\
&\mathcal{V}^{T}_{\alpha,\beta,\gamma}F\mathfrak{L}^{\mu,a,b}_{\alpha,\beta,\gamma}(t_{\mu,\rho},x_{a,\upsilon},0)=\nu_2(t_{\mu,\rho},x_{a,\upsilon}), && 1\le\rho\le\alpha,\quad 1\le\upsilon\le\beta-1,\\
&\mathcal{U}^{T}_{\alpha,\beta,\gamma}F\mathfrak{L}^{\mu,a,b}_{\alpha,\beta,\gamma}(t_{\mu,\rho},x_{a,\upsilon},b)=\sigma_1(t_{\mu,\rho},x_{a,\upsilon}), && 1\le\rho\le\alpha,\quad 1\le\upsilon\le\beta-1,\\
&\mathcal{V}^{T}_{\alpha,\beta,\gamma}F\mathfrak{L}^{\mu,a,b}_{\alpha,\beta,\gamma}(t_{\mu,\rho},x_{a,\upsilon},b)=\sigma_2(t_{\mu,\rho},x_{a,\upsilon}), && 1\le\rho\le\alpha,\quad 1\le\upsilon\le\beta-1,
\end{aligned}\tag{4.10}$$

where $(t_{\mu,\rho},x_{a,\upsilon},y_{b,\tau})$ are the roots of the two-dimensional FSLF. The essential computational steps of the proposed collocation formulation are summarized in Algorithm 2, which provide a clear procedural outline of the implementation.

Algorithm 2: Two-dimensional FSLF collocation scheme

Step 1	Fix $0<\mu\le 1$, d_u, d_v, F, K, domain lengths a, b, and truncation indices α,β,γ.
Step 2	Construct the 2D FSLF basis $F\mathfrak{L}^{\mu,a,b}_{\alpha,\beta,\gamma}(t,x,y)$ using (2.6).
Step 3	Assemble the operational matrices $\mathcal{S}^{x,2,a,b}_{\alpha,\beta,\gamma}$, $\mathcal{S}^{y,2,a,b}_{\alpha,\beta,\gamma}$, $\mathcal{Q}^{\mu,a,b}_{\alpha,\beta,\gamma}$ from Theorems 5–7.
Step 4	Choose collocation nodes $(t_{\mu,\rho},x_{a,\upsilon},y_{b,\tau})$ as the roots of $F\mathfrak{L}^{\mu,a,b}_{\alpha+1,\beta+1,\gamma+1}(t,x,y)$ and add boundary points.
Step 5	Express $u_{\alpha,\beta,\gamma}, v_{\alpha,\beta,\gamma}$ as in (4.3), form the residuals ${}^1\mathcal{R}_{\alpha,\beta,\gamma}$, ${}^2\mathcal{R}_{\alpha,\beta,\gamma}$, collocate them using (4.9), and impose the boundary/initial conditions (4.10) to obtain the full algebraic system.
Step 6	Solve the resulting nonlinear algebraic system for $\mathcal{U}_{\alpha,\beta,\gamma}$ and $\mathcal{V}_{\alpha,\beta,\gamma}$, and reconstruct the numerical solutions $u_{\alpha,\beta,\gamma}(t,x,y)$, $v_{\alpha,\beta,\gamma}(t,x,y)$ using (4.3).

5. Numerical results

In all numerical experiments, the nonlinear algebraic system is solved using the built-in FindRoot solver in Mathematica, where the nonlinear terms are evaluated explicitly within the residual formulation.

Example 1. *As the first example, we consider the model* (3.1) *and* (3.2) *with* $d_u=\dfrac{2}{100,000}$, $d_v=\dfrac{1}{100,000}$, $F=\dfrac{3}{100,000}$, $K=\dfrac{55}{100,000}$,

$$\begin{aligned}
g_1(t,x)&=\Gamma(\mu+1)\cos(x)+d_u t^{\mu}\cos(x)+t^{3\mu}\cos(x)e^{-2x}-F+Ft^{\mu}\cos(x),\\
g_2(t,x)&=\Gamma(\mu+1)e^{-x}-d_v t^{\mu}e^{-x}-t^{3\mu}\cos(x)e^{-2x}+(F-K)t^{\mu}e^{-x},
\end{aligned}\tag{5.1}$$

and the exact solution is given as $(u(t,x), v(t,x)) = (t^{\mu}\cos(x), t^{\mu}e^{-x})$. *We apply the numerical scheme discussed in Section 3 to solve this model with* $\alpha = \{3, 10\}$ *and different values of* β. *Table 1 displays the maximum absolute errors (MAEs) of* $u(t,x)$ *and* $v(t,x)$ *with* $\alpha = 3$ *at* $\mu = \{0.3, 0.6, 0.9\}$. *Table 2 obtains the maximum absolute errors of* $u(t,x)$ *and* $v(t,x)$ *with* $\alpha = 10$ *at* $\mu = \{0.25, 0.50, 0.75\}$. *To study the performance of the presented numerical approach when the fractional order* μ *approaches the two ends, in Table 3, we display the MAEs of* $u(t,x)$ *and* $v(t,x)$ *with* $\alpha = 3$ *at* $\mu = \{0.01, 0.99\}$. *Figures 1 and 2 display the temporal and spacial absolute errors of* $u(t,x)$ *and* $v(t,x)$, *respectively, at* $\mu = 0.5$ *with* $(\alpha, \beta) = (3, 15)$. *Figures 3 and 4 display contour plots of absolute errors of* $u(t,x)$ *and* $v(t,x)$, *respectively, at* $\mu = 0.5$ *with* $\alpha = 3$ *and* $\beta = \{5, 10, 15\}$. *The numerical results shown in Tables 1–3 and Figures 1–4 confirm the high accuracy and convergence of the presented numerical approach with different choices of the parameters* α *and* β *at any value of* $\mu \in (0, 1)$, *and when* μ *approaches the two ends.*

Table 1. MAEs with $\alpha = 3$ for Example 1.

	$\mu = 0.3$		$\mu = 0.6$		$\mu = 0.9$	
β	$u(t,x)$	$v(t,x)$	$u(t,x)$	$v(t,x)$	$u(t,x)$	$v(t,x)$
3	1.084×10^{-2}	1.447×10^{-2}	1.084×10^{-2}	1.447×10^{-2}	1.084×10^{-2}	1.446×10^{-2}
6	1.238×10^{-4}	3.370×10^{-5}	1.238×10^{-4}	3.371×10^{-5}	1.238×10^{-4}	3.371×10^{-5}
9	1.241×10^{-8}	2.444×10^{-8}	1.239×10^{-8}	2.442×10^{-8}	1.238×10^{-8}	2.441×10^{-8}
12	3.192×10^{-11}	6.498×10^{-12}	3.190×10^{-11}	6.501×10^{-12}	3.188×10^{-11}	6.500×10^{-12}
15	1.443×10^{-15}	1.373×10^{-15}	1.332×10^{-15}	1.373×10^{-15}	1.554×10^{-15}	1.429×10^{-15}

Table 2. MAEs with $\alpha = 10$ for Example 1.

	$\mu = 0.25$		$\mu = 0.50$		$\mu = 0.75$	
β	$u(t,x)$	$v(t,x)$	$u(t,x)$	$v(t,x)$	$u(t,x)$	$v(t,x)$
4	7.242×10^{-3}	2.279×10^{-3}	7.243×10^{-3}	2.280×10^{-3}	7.242×10^{-3}	2.279×10^{-3}
8	1.185×10^{-6}	3.260×10^{-7}	1.186×10^{-6}	3.248×10^{-7}	1.187×10^{-6}	3.244×10^{-7}
12	3.193×10^{-11}	6.496×10^{-12}	3.191×10^{-11}	6.502×10^{-12}	3.189×10^{-11}	6.503×10^{-12}
16	1.110×10^{-15}	1.589×10^{-15}	9.992×10^{-16}	1.630×10^{-15}	1.110×10^{-15}	1.526×10^{-15}

Table 3. MAEs with $\alpha = 3$ at $\mu = 0.01$ and $\mu = 0.99$ for Example 1.

	$\mu = 0.99$		$\mu = 0.01$	
β	$u(t,x)$	$v(t,x)$	$u(t,x)$	$v(t,x)$
3	1.084×10^{-2}	1.447×10^{-2}	1.084×10^{-2}	1.446×10^{-2}
6	1.239×10^{-4}	3.370×10^{-5}	1.238×10^{-4}	3.372×10^{-5}
9	1.244×10^{-8}	2.447×10^{-8}	1.238×10^{-8}	2.441×10^{-8}
12	3.194×10^{-11}	6.492×10^{-12}	3.188×10^{-11}	6.501×10^{-12}
15	1.221×10^{-15}	1.277×10^{-15}	9.992×10^{-16}	1.290×10^{-15}

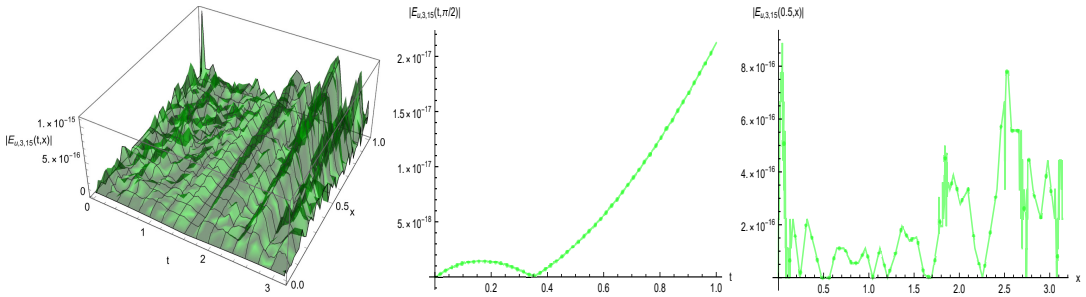

Figure 1. Absolute errors of $u(t, x)$ at $\mu = 0.5$ with $(\alpha, \beta) = (3, 15)$ for Example 1.

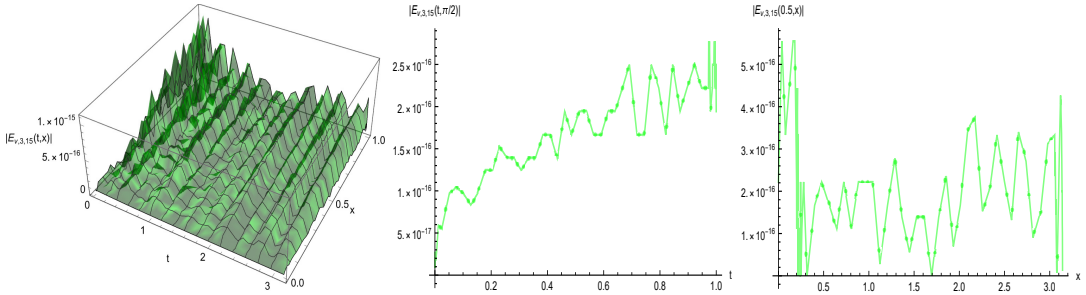

Figure 2. Absolute errors of $v(t, x)$ at $\mu = 0.5$ with $(\alpha, \beta) = (3, 15)$ for Example 1.

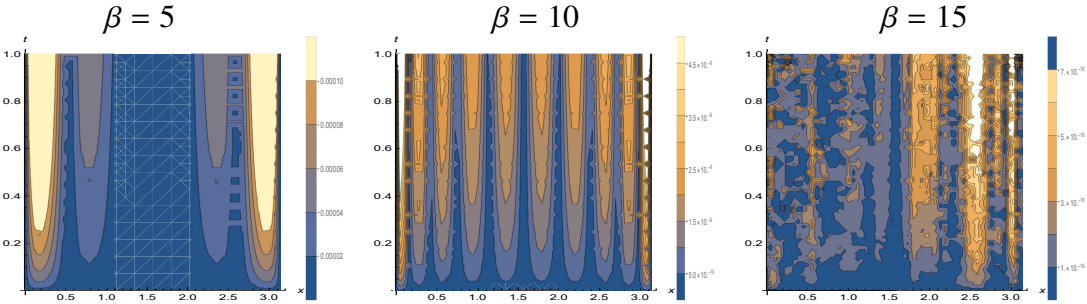

Figure 3. Contour plot of AEs of $u(t, x)$ at $\mu = 0.5$ with $\alpha = 3$ for Example 1.

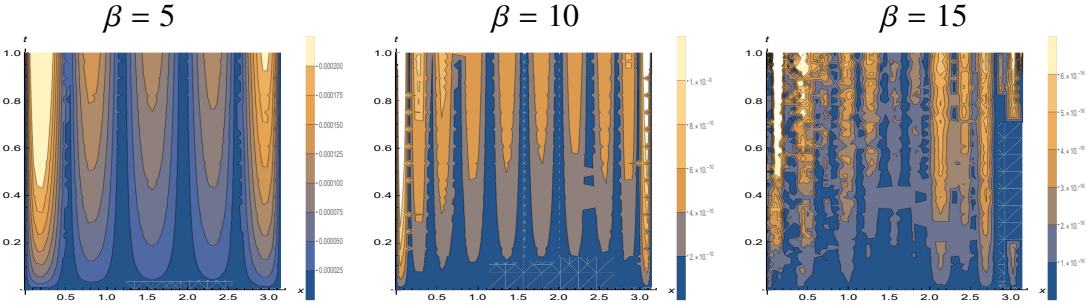

Figure 4. Contour plot of AEs of $v(t, x)$ at $\mu = 0.5$ with $\alpha = 3$ for Example 1.

Example 2. *To evaluate the convergence behavior of the proposed numerical method, we consider the model* (3.1) *and* (3.2) *with* $d_u = \frac{2}{100,000}$, $d_v = \frac{1}{100,000}$, $F = \frac{3}{100,000}$, $K = \frac{63}{100,000}$, *and the exact solution is* $(u(t,x), v(t,x)) = \left(t^{\mu+1}\sin(2x), t^{\mu+2}\cos 2x\right)$. *Here, we apply the presented numerical scheme with* $\alpha = \{5, 10\}$ *and different values of* β. *İn Table 4, we list the MAEs of* $u(t,x)$ *and* $v(t,x)$ *with* $\alpha = \{5, 10\}$ *at* $\mu = 0.5$, *and with* $\alpha = 10$ *at* $\mu = 0.5$, *Moreover, in Figure 5, we plot the logarithmic function of MAEs of* $u(t,x)$ *and* $v(t,x)$ *to show the convergence with various choices of* β. *The numerical results shown in Table 4 and Figure 5 confirm that the MAEs of the approximate solution decrease with increasing values of* β, *ensuring the high convergence and accuracy of the considered approach.*

Table 4. MAEs with $\alpha = 10$ at $\mu = 0.25$ and $\mu = 0.50$ for Example 2.

	$\mu = 0.25$		$\mu = 0.50$	
β	$u(t,x)$	$v(t,x)$	$u(t,x)$	$v(t,x)$
2	9.99574×10^{-1}	6.10910×10^{-1}	9.99573×10^{-1}	6.10906×10^{-1}
4	1.61084×10^{-1}	8.05343×10^{-2}	1.61083×10^{-1}	8.05331×10^{-2}
6	1.21021×10^{-2}	4.65860×10^{-3}	1.21017×10^{-2}	4.65851×10^{-3}
8	4.92741×10^{-4}	1.52229×10^{-4}	4.92774×10^{-4}	1.52116×10^{-4}
10	1.17925×10^{-5}	3.10444×10^{-6}	1.17912×10^{-5}	3.10540×10^{-6}
12	2.25746×10^{-7}	5.03645×10^{-8}	2.25702×10^{-7}	5.04175×10^{-8}
14	2.82727×10^{-9}	5.45819×10^{-10}	2.82629×10^{-9}	5.47399×10^{-10}
16	2.39269×10^{-11}	4.03710×10^{-12}	2.39114×10^{-11}	4.06608×10^{-12}
18	1.79092×10^{-13}	3.43058×10^{-14}	1.79703×10^{-13}	3.05311×10^{-14}

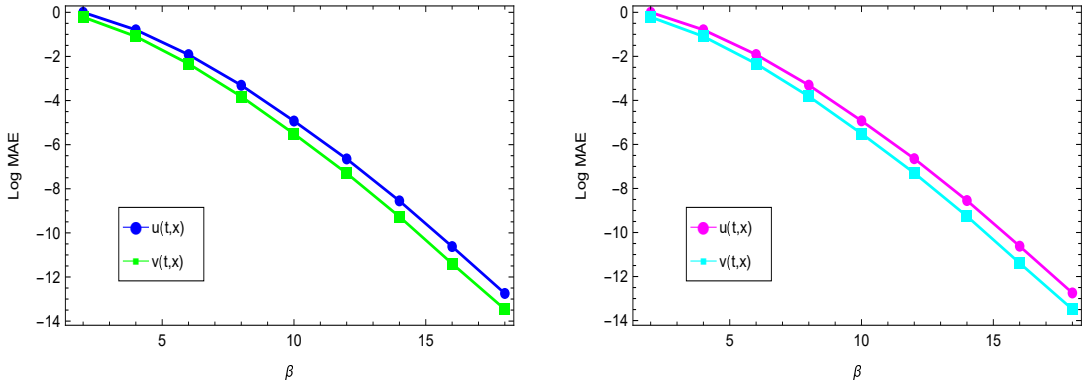

Figure 5. Convergence of $u(t,x)$ and $v(t,x)$ at $\mu = 0.25$ (left) and $\mu = 0.50$ (right) with $\alpha = 10$ for Example 2.

Example 3. *Now, we consider the time-fractional Gray-Scott model* (4.1) *and* (4.2) *with* $d_u = \frac{2}{100,000}$, $d_v = \frac{1}{100,000}$, $F = \frac{3}{100,000}$, $K = \frac{55}{100,000}$, *and* $g_1(t,x,y)$ *and* $g_2(t,x,y)$ *are chosen so that the exact solution is* $(u(t,x,y), v(t,x,y)) = ((t^{\mu} + t^{2\mu} + t^2)\sin(\pi x)\sin(\pi y), -(t^{\mu} + t^{2\mu})\sin(\pi x)\sin(\pi y))$. *Deng et al. [31] considered this model with* $\mu = 0.4$ *and* 0.6, *and implemented a high-order fitted scheme*

based on the L2-1$_\sigma$ for its solution. We test our numerical method to solve the current model with $\alpha = 9$ and $\beta = \gamma = \{3, 6, 9\}$, and compare the given outputs against those in [31] in Table 5. Figures 6 and 7 display comparisons between the exact solutions and approximate solutions of $u(t, x, y)$ and $v(t, x, y)$, respectively, at $\mu = 0.4$ with $(\alpha, \beta, \gamma) = (9, 9, 9)$. Figures 8 and 9 display comparisons between the exact solutions and approximate solutions of $u(t, x, y)$ and $v(t, x, y)$, respectively, at $\mu = 0.6$ with $(\alpha, \beta, \gamma) = (9, 9, 9)$. Figures 10 and 11 display the temporal and spacial absolute errors of $u(t, x, y)$ and $v(t, x, y)$, respectively, at $\mu = 0.5$ with $(\alpha, \beta, \gamma) = (9, 9, 9)$.

Table 5. Comparing absolute errors versus the method in [31] for Example 3.

	Method in [31] ($h = 1/100$)			FSLFs Basis		
μ	N	$E_u(t, x, y)$	$E_v(t, x, y)$	$\beta = \gamma$	$E_u(t, x, y)$	$E_v(t, x, y)$
	512	1.2937×10^{-5}	1.2937×10^{-5}	3	1.5829×10^{-1}	1.0556×10^{-1}
0.4	1024	6.4674×10^{-6}	6.4674×10^{-6}	6	2.6394×10^{-5}	1.7502×10^{-5}
	2048	3.2334×10^{-6}	3.2334×10^{-6}	9	2.0741×10^{-7}	1.3849×10^{-7}
	512	1.1823×10^{-5}	1.1823×10^{-5}	3	1.5830×10^{-1}	1.0556×10^{-1}
0.6	1024	5.9127×10^{-6}	5.9127×10^{-6}	6	2.6467×10^{-5}	1.7492×10^{-5}
	2048	2.9567×10^{-6}	2.9567×10^{-6}	9	1.1456×10^{-6}	2.5552×10^{-7}

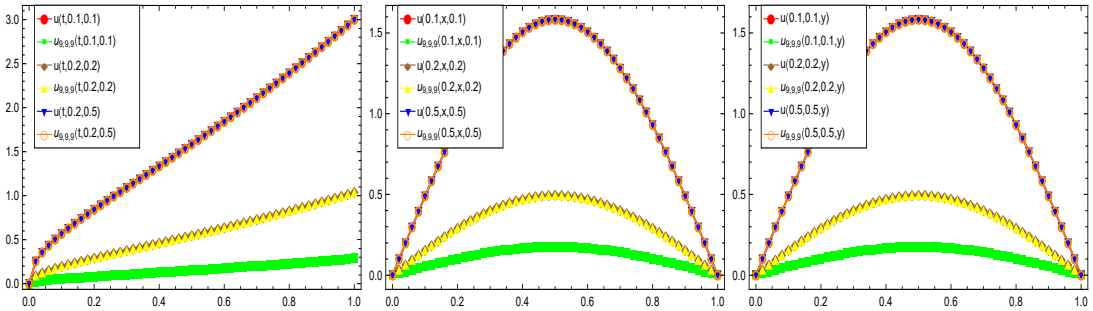

Figure 6. Exact and approximate solutions of $u(t, x, y)$ at $\mu = 0.4$ and $(\alpha, \beta, \gamma) = (9, 9, 9)$ for Example 3.

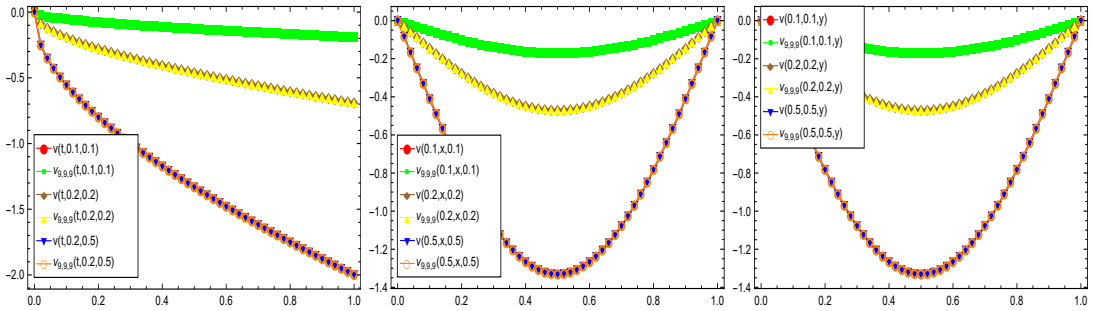

Figure 7. Exact and approximate solutions of $v(t, x, y)$ at $\mu = 0.4$ and $(\alpha, \beta, \gamma) = (9, 9, 9)$ for Example 3.

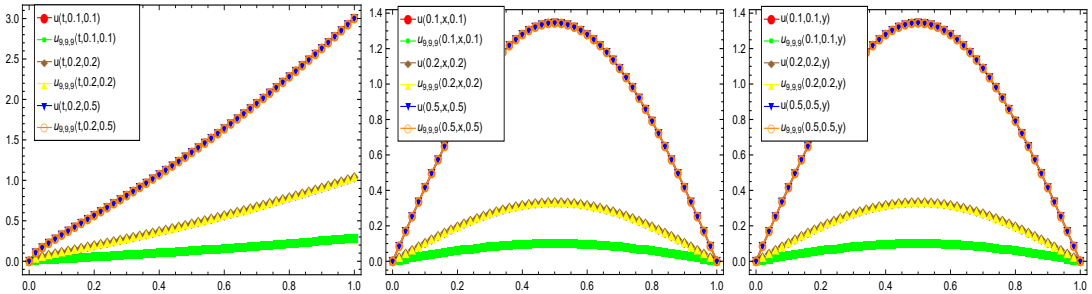

Figure 8. Exact and approximate solutions of $u(t, x, y)$ at $\mu = 0.6$ and $(\alpha, \beta, \gamma) = (9, 9, 9)$ for Example 3.

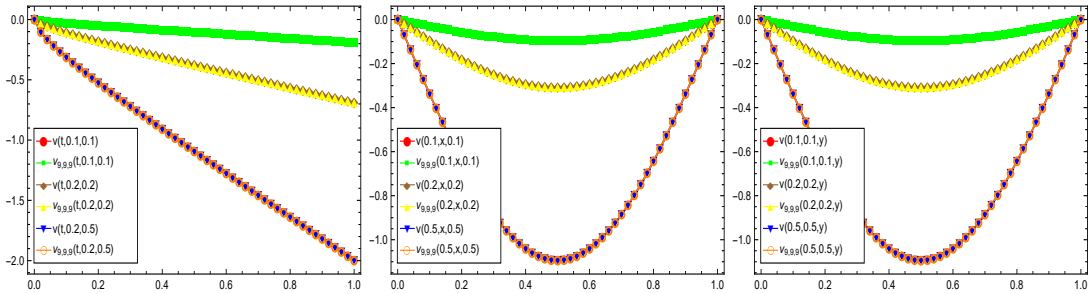

Figure 9. Exact and approximate solutions of $v(t, x, y)$ at $\mu = 0.6$ and $(\alpha, \beta, \gamma) = (9, 9, 9)$ for Example 3.

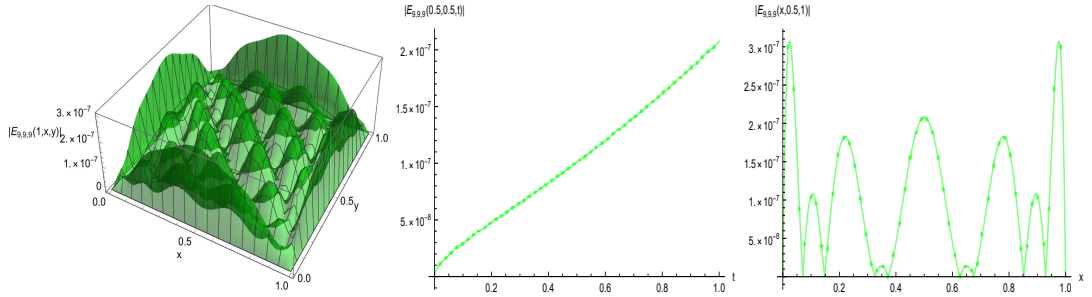

Figure 10. Absolute errors of $u(t, x, y)$ at $\mu = 0.5$ and $(\alpha, \beta, \gamma) = (9, 9, 9)$ for Example 3.

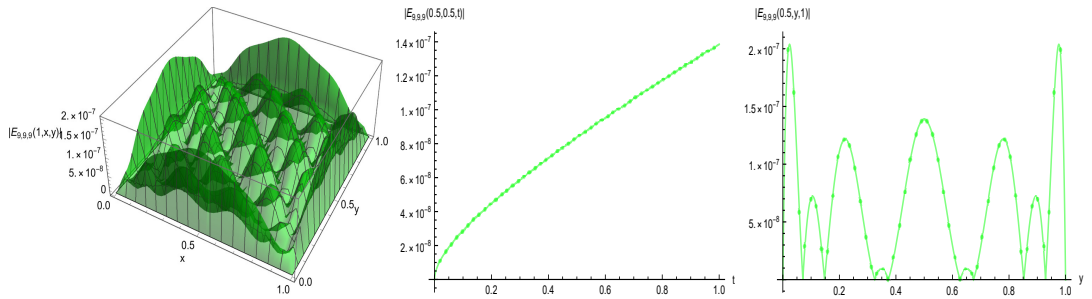

Figure 11. Absolute errors of $v(t, x, y)$ at $\mu = 0.5$ and $(\alpha, \beta, \gamma) = (9, 9, 9)$ for Example 3.

Example 4. *The current problem is devoted to confirming the superiority of the proposed numerical approach over other existing approaches. We consider the model* (4.1) *and* (4.2) *with* $d_u = \dfrac{2}{100,000}$, $d_v = \dfrac{1}{100,000}$, $F = \dfrac{3}{100}$, $K = \dfrac{63}{1000}$, *and*

$$\begin{aligned} g_1(t,x,y) &= 2d_u t^2(x - x^2 + y - y^2) - F + 2txy(x-1)(y-1) + Ft^2xy(x-1)(y-1) \\ &\quad + t^2x^5y^5e^{-2t}(x-1)^5(y-1)^5, \\ g_2(t,x,y) &= 8x^2ye^{-t}(y-1)(x-1)^2) + 8xy^2e^{-t}(x-1)(y-1)^2 + 2y^2e^{-t}(x-1)^2(y-1)^2 \\ &\quad - t^2x^5y^5e^{-2t}(x-1)^5(y-1)^5 - x^2y^2e^{-t}(x-1)^2(y-1)^2 + x^2y^2e^{-t}(x-1)^2(y-1)^2(F+K) \\ &\quad + 2x^2e^{-t}(x-1)^2(y-1)^2 + 2x^2y^2e^{-t}(y-1)^2 - d_v(2x^2y^2e^{-t}(x-1)^2, \end{aligned}$$

where the exact solution is $(u(t,x,y), v(t,x,y)) = (t^2(x-x^2)(y-y^2), e^{-t}x^2(1-x)^2y^2(1-y)^2)$. *The current problem was introduced by Sakariya and Kumar [23] who found its numerical solution utilizing the finite difference approximation and radial basis functions (RBFs)-based collocation method for time and space directions, respectively. In Table 6, we compare the MAEs of* $u(t,x,y)$ *and* $v(t,x,y)$ *versus those given using the RBFs by Sakariya and Kumar [23].*

The numerical results shown in Table 6 indicate that the MAE of the numerical solution achieved using the proposed method is lower than that achieved using the RBF approach [23] with low degrees of basis functions. This ensures high accuracy and rapid convergence of our numerical scheme compared with the RBF approach [23].

Table 6. Comparing MAEs of $u(t,x,y)$ and $v(t,x,y)$ versus the RBFs in [23] for Example 4.

RBFs [23] ($\delta t = 1/100$)				FSLFs Basis			
$n = m$	t	$u(t,x,y)$	$v(t,x,y)$	$\alpha = \beta = \gamma$	t	$u(t,x,y)$	$v(t,x,y)$
	0.2	1.2500×10^{-4}	1.1406×10^{-5}		0.2	1.5380×10^{-9}	3.3022×10^{-3}
	0.4	2.5000×10^{-4}	9.3883×10^{-6}		0.4	1.4680×10^{-8}	3.1709×10^{-3}
11	0.6	3.7499×10^{-4}	7.7363×10^{-6}	3	0.6	4.0643×10^{-8}	2.5674×10^{-3}
	0.8	4.9998×10^{-4}	9.3356×10^{-6}		0.8	8.0644×10^{-8}	1.9474×10^{-3}
	1.0	6.2496×10^{-4}	1.0590×10^{-5}		1.0	1.3590×10^{-7}	1.8141×10^{-3}
	0.2	1.2446×10^{-4}	2.4924×10^{-5}		0.2	3.3975×10^{-13}	1.7601×10^{-8}
	0.4	2.4581×10^{-4}	1.8451×10^{-5}		0.4	9.7498×10^{-13}	1.6888×10^{-8}
31	0.6	3.6105×10^{-4}	1.3189×10^{-5}	6	0.6	2.4481×10^{-12}	1.6684×10^{-8}
	0.8	4.6720×10^{-4}	8.9156×10^{-6}		0.8	4.6867×10^{-12}	1.6318×10^{-8}
	1.0	5.6129×10^{-4}	6.9746×10^{-6}		1.0	7.6987×10^{-12}	1.6015×10^{-8}
	0.2	1.2015×10^{-4}	6.3732×10^{-6}		0.2	1.2886×10^{-16}	6.1709×10^{-13}
	0.4	2.1267×10^{-4}	1.1456×10^{-5}		0.4	1.3995×10^{-16}	6.0919×10^{-13}
41	0.6	2.5089×10^{-4}	1.5486×10^{-5}	9	0.6	1.6046×10^{-16}	6.1338×10^{-13}
	0.8	2.0846×10^{-4}	1.8656×10^{-5}		0.8	2.0530×10^{-16}	5.9751×10^{-13}
	1.0	5.9316×10^{-5}	2.1126×10^{-5}		1.0	7.0983×10^{-16}	5.8465×10^{-13}

6. Conclusions

In this work, we have presented an efficient numerical solution for one- and two-dimensional time-fractional Gray-Scott models. We have formulated a new set of basis function, one- and two-dimensional fractional-order shifted Legendre functions, to be used as the basis for an operational matrix technique combined with the spectral collocation method to simplify the model into a system of algebraic equations. New operational matrices have been derived based on the new basis functions. To our knowledge, this work has presented the first attempt to introduce an operational matrix of fractional-order derivatives exactly in the basis used. Numerical results have confirmed that using the operational matrix method with the spectral collocation method, based on non-smooth basis functions in the time-direction, to solve time-fractional partial differential equations yields efficient and accurate results compared to these methods when applied based on smooth basis functions.

Author contributions

Samer S. Ezz-Eldien: Writing–review and editing, writing–original draft, validation, supervision, software, investigation; Ali H. Tedjani: Validation, methodology, writing the original draft; Amra Al Kenany: Software, investigation; Marwa Alzubaidi: Software, investigation. All authors have read and agreed to the published version of the manuscript.

Use of Generative-AI tools declaration

The authors declare they have not used Artificial Intelligence (AI) tools in the creation of this article.

Acknowledgments

This work was supported and funded by the Deanship of Scientific Research at Imam Mohammad Ibn Saud Islamic University (IMSIU) (grant number IMSIU-DDRSP2601).

Conflicts of interest

The authors declare that they have no conflicts of interest.

References

1. A. N. Landge, B. M. Jordan, X. Diego, P. Müller, Pattern formation mechanisms of self-organizing reaction-diffusion systems, *Dev. Biol.*, **460** (2020), 2–11. https://doi.org/10.1016/j.ydbio.2019.10.031
2. N. Luo, S. Wang, L. You, Synthetic pattern formation, *Biochemistry*, **58** (2019), 1478–1483. https://doi.org/10.1021/acs.biochem.8b01242
3. S. S. Ezz-Eldien, On solving fractional logistic population models with applications, *Comput. Appl. Math.*, **37** (2018), 6392–6409. https://doi.org/10.1007/s40314-018-0693-4

4. J. S. Moreno, Y. Schaerli, Using synthetic biology to engineer spatial patterns, *Adv. Biosyst.*, **3** (2019), 1800280. https://doi.org/10.1002/adbi.201800280
5. M. A. Zaky, A linearized two-dimensional Galerkin–L1 spectral method with diagonalization for time-fractional diffusion equations with delay, *Appl. Numer. Math.*, **220** (2026), 1–12. https://doi.org/10.1016/j.apnum.2025.09.008
6. R. G. Coss, E. P. Charles, The saliency of snake scales and leopard rosettes to infants: Its relevance to graphical patterns portrayed in prehistoric art, *Front. Psychol.*, **12** (2021), 1–11. https://doi.org/10.3389/fpsyg.2021.763436
7. A. M. Turing, The chemical basis of morphogenesis, *B. Math. Biol.*, **52** (1990), 153–197. https://doi.org/10.1098/rstb.1952.0012
8. K. Wang, W. Wang, Propagation of HBV with spatial dependence, *Math. Biosci.*, **210** (2007), 78–95. https://doi.org/10.1016/j.mbs.2007.05.004
9. T. Fromenteze, O. Yurduseven, C. Uche, E. Arnaud, D. R. Smith, C. Decroze, Morphogenetic metasurfaces: Unlocking the potential of Turing patterns, *Nat. Commun.*, **14** (2023), 6249. https://doi.org/10.1038/s41467-023-41775-9
10. F. Giampaolo, M. D. Rosa, P. Qi, S. Izzo, S. Cuomo, Physics-informed neural networks approach for 1D and 2D Gray-Scott systems, *Adv. Model. Simul. Eng.*, **9** (2022), 5. https://doi.org/10.1186/s40323-022-00219-7
11. E. Pindza, K. M. Owolabi, Fourier spectral method for higher order space fractional reaction–diffusion equations, *Commun. Nonlinear Sci.*, **40** (2016), 112–128. https://doi.org/10.1016/j.cnsns.2016.04.020
12. M. Alqhtani, K. M. Owolabi, K. M. Saad, Spatiotemporal (target) patterns in sub-diffusive predator-prey system with the Caputo operator, *Chaos Soliton. Fract.*, **160** (2022), 112267. https://doi.org/ 10.1016/j.chaos.2022.112267
13. M. Alqhtani, K. M. Owolabi, K. M. Saad, E. Pindza, Efficient numerical techniques for computing Riesz fractional-order reaction-diffusion models arising in biology, *Chaos Soliton. Fract.*, **161** (2022), 112394. https://doi.org/ 10.1016/j.chaos.2022.112394
14. R. M. Hafez, S. S. Ezz-Eldien, A. H. Bhrawy, E. A. Ahmed, D. Baleanu, A Jacobi Gauss-Lobatto and Gauss-Radau collocation algorithm for solving fractional Fokker-Planck equations, *Nonlinear Dynam.*, **82** (2015), 1431–1440. https://doi.org/ 10.1007/s11071-015-2250-7.
15. M. M. Alsuyuti, E. H. Doha, S. S. Ezz-Eldien, Numerical simulation for classes of one- and two-dimensional multi-term time-fractional diffusion and diffusion-wave equation based on shifted Jacobi Galerkin scheme, *Math. Method. Appl. Sci.*, **48** (2025), 8217–8244. https://doi.org/10.1002/mma.9659
16. G. S. Yi, J. Wang, X. L. Wei, B. Deng, Dynamics of spike threshold in a two-compartment neuron with passive dendrite, *Commun. Nonlinear Sci.*, **40** (2016), 100–111. https://doi.org/10.1016/j.cnsns.2016.04.021
17. C. Han, X. Lu, Novel patterns in the space variable fractional order Gray-Scott model, *Nonlinear Dynam.*, **112** (2024), 16135–16151. https://doi.org/10.1007/s11071-024-09857-5

18. S. Momani, I. M. Batiha, I. Bendib, A. Ouannas, A. Hioual, D. Mohamed, Examining finite-time behaviors in the fractional Gray-Scott model: Stability, synchronization, and simulation analysis, *Int. J. Cogn. Comput. Eng.*, **6** (2025), 380–390. https://doi.org/10.1016/j.ijcce.2025.02.004

19. T. Wang, F. Song, H. Wang, G. E. Karniadakis, Fractional Gray-Scott model: Well-posedness, discretization, and simulations, *Comput. Method. Appl. M.*, **347** (2019), 1030–1049. https://doi.org/10.1016/j.cma.2019.01.002

20. C. Han, Y. L. Wang, Z. Y. Li, A high-precision numerical approach to solving space fractional Gray-Scott model, *Appl. Math. Lett.*, **125** (2022), 107759. https://doi.org/10.1016/j.aml.2021.107759

21. L. Chai, Y. Liu, H. Li, W. Gao, Fast TT-M fourth-order compact difference schemes for a two-dimensional space fractional Gray-Scott model, *Comput. Math. Appl.*, **141** (2023), 191–206. https://doi.org/ 10.1016/j.camwa.2023.04.039

22. S. Aljhani, M. S. MD, K. M. Saad, A. K. Alomari, Numerical solutions of certain new models of the time-fractional Gray-Scott, *J. Funct. Space.*, **2021** (2021), 2544688. https://doi.org/10.1155/2021/2544688

23. H. Sakariya, S. Kumar, Numerical simulation of the time fractional Gray-Scott model on 2D space domains using radial basis functions, *J. Math. Chem.*, **62** (2024), 836–864. https://doi.org/10.1007/s10910-023-01571-8

24. M. A. Zaky, O. A. Arqub, Improved spectral method for the nonsmooth solutions of nonlinear fractional differential equations, *J. Appl. Math. Comput.*, **71** (2025), 9173–9190. https://doi.org/10.1007/s12190-025-02633-7

25. M. A. Zaky, I. G. Ameen, O. A. Arqub, E. H. Doha, High-order fractional spectral collocation method for the nonsmooth solutions of nonlinear right-sided Caputo terminal value problems, *Fract. Calc. Appl. Anal.*, **28** (2025), 3189–3210. https://doi.org/10.1007/s13540-025-00464-8

26. A. H. Bhrawy, M. A. Zaky, Shifted fractional-order Jacobi orthogonal functions: Application to a system of fractional differential equations, *Appl. Math. Model.*, **40** (2016), 832–845. https://doi.org/10.1016/j.apm.2015.06.012

27. M. A. Zaky, E. H. Doha, J. A. T. Machado, A spectral framework for fractional variational problems based on fractional Jacobi functions, *Appl. Numer. Math.*, **132** (2018), 51–72. https://doi.org/10.1016/j.apnum.2018.05.009

28. H. Moussa, M. A. Saker, M. A. Zaky, M. Babatin, S. S. Ezz-Eldien, Mapped Legendre-spectral method for high-dimensional multi-term time-fractional diffusion-wave equation with non-smooth solution, *Comput. Appl. Math.*, **44** (2025), 167. https://doi.org/ 10.1007/s40314-025-03123-z

29. S. S. Ezz-Eldien, E. H. Doha, Y. Wang, W. Cai, A numerical treatment of the two-dimensional multi-term time-fractional mixed sub-diffusion and diffusion-wave equation, *Commun. Nonlinear Sci.*, **91** (2021), 105445. https://doi.org/10.1016/j.cma.2025.115161

30. E. H. Doha, Explicit formulae for the coefficients of integrated expansions of Jacobi polynomials and their integrals, *Integr. Transf. Spec. F.*, **14** (2003), 69–86. https://doi.org/10.1080/10652460304541

31. X. Deng, C. Ou, Z. Wang, S. Vong, A fitted scheme for the nonlinear time fractional Gray-Scott model with nonsmooth solutions, *J. Appl. Math. Comput.*, **71** (2025), 6621–6650. https://doi.org/10.1007/s12190-025-02552-7

AIMS Press